# PERFORMANCE EVALUATION OF HIGH-RATE STBC COMMUNICATION SYSTEM USING IMPERFECT CSI WORKING UNDER TIME-SELECTIVE FLAT-FADING CHANNEL

Submitted towards the partial fulfilment of requirement for the award of degree of

**Master of Engineering**

**In**

**Wireless Communication**


Submitted by:

**SONALI**

**(801463027)**

Under the guidance of:

**Dr. Amit Kumar Kohli**

**(Associate Professor, ECED)**



**ELECTRONICS AND COMMUNICATION ENGINEERING DEPARTMENT**

**THAPAR UNIVERSITY**

**(Established under the section 3 of UGC Act, 1956)**

**PATIALA – 147004, PUNJAB, INDIA**



**JULY 2016**

# DECLARATION

I, **Sonali**, hereby declare that the thesis entitled **"Performance Evaluation of High-Rate STBC Communication System Using Imperfect CSI Working Under Time-Selective Flat-Fading Channel"** is an authentic record of my own work carried out towards the partial fulfillment for the award of the degree of Master of Engineering in Wireless Communication at Thapar University, Patiala under the guidance of **Dr. Amit Kumar Kohli**, Associate Professor, Electronics and Communication Engineering Department.

The matter presented in this thesis has not been submitted in any other University/Institute for the award of any other degree.

Sonali

Date: 02/07/2016

**Sonali**
Roll No. 801463027

This is to certify that the above statement made by the student is correct to the best of my knowledge and belief.

Amit Kohli 2/7/16

Date:

**Dr. Amit Kumar Kohli**
Associate Professor, ECED
Thapar University, Patiala

Countersigned by:

**(Dr. Sanjay Sharma)**
Professor and Head ECED
Thapar University, Patiala

**(Dr. S. S. Bhatia)**
Dean of Academic Affairs
Thapar University, Patiala

# ACKNOWLEDGEMENT

Foremost, I would like to express my sincere gratitude to my guide **Dr. Amit Kumar Kohli**, Associate Professor and P.G. Coordinator, ECED, Thapar University, Patiala, for his patience, motivation, enthusiasm, immense knowledge and continuous support for my thesis. His guidance helped me in research and writing of this thesis all the time. I could not have imagined having a better guidance for my thesis.

Besides my guide, I am thankful to **Dr. Sanjay Sharma**, Professor and Head, Electronics and Communication Engineering Department and **Dr. Hemdutt Joshi**, Assistant Professor, Program Coordinator of Wireless Communication, who have been a consistent source of inspiration for me throughout this work, and for providing us with adequate infrastructure in carrying out my work.

I would like to thank all the faculty members of ECED for their full support for my work. I am also thankful to my friends **Shivani Sehrawat, Rohit Garg and Shiv Kumar Sharma**, for encouraging the use of correct grammar and consistent notation in my writings and for carefully reading and commenting on countless revisions of my manuscript. I am also thankful to the authors whose work have been consulted and quoted in this work.

At last but not the least, I would also like to thank my parents for supporting me throughout my life.

Place: Thapar University, Patiala — Sonali

Date: — Roll No.: 801463027

# ABSTRACT

Multi-input-multi-output (MIMO) system employs multiple antennas at both sides of the link, which enhances transmit diversity and provides better reliability. An orthogonal-space-time-block-coding (O-STBC) scheme has been first proposed by Alamouti, for achieving maximum diversity gain for two transmitting antennas. It also attains the full rate as well as full diversity gain. In addition to this, O-STBC scheme was proposed for more than two transmitting antennas to attain full diversity gain (Tarokh *et al.*, 1999). However, the scheme could not achieve the full rate. To overcome this, a quasi-orthogonal-space-time-block-coding (QO-STBC) scheme was proposed by Jafarkhani (Jafarkhani, 2001). In practical scenario, channel coefficients in the wireless transmission varies due to Doppler spread and local oscillator frequency mismatch between transmitter and receiver, i.e., carrier-frequency-offset (CFO). To analyze the time-selective channels, these are modelled as an autoregressive (AR) process.

This work discusses high-rate transmission scheme under time-selective fading channel in terms of symbol-error-rate (SER) and the effective throughput performance under the perfect channel state information (CSI). As, it is not practically possible for channel estimator to estimate the channel without errors, so the proposed schemes has also been analyzed under the imperfect CSI at the receiver side. This analysis uses Rayleigh flat-fading channel.

Here, we evaluate the performance of high-rate $(5/4)$ space-time-block-coding (STBC) system working under time-selective flat-fading channel in the presence of channel estimation errors. For the performance evaluation of high-rate $(9/8)$ STBC system, we have considered time-nonselective flat-fading channel in the presence of channel estimation errors. The STBC high-rate $(5/4)$ and $(9/8)$ are achieved using two transmitter and four transmitter antennas respectively. Both the schemes use selective power scaling in combination with quadrature-phase-shift-keying (QPSK) modulation technique. The main focus is on the impact of CFO and Doppler spread on the SER and effective throughput performance of the underlying STBC system. Simulation results are presented to illustrate that the proposed high-rate $(5/4)$ and $(9/8)$ STBC systems perform well only under the high signal-to-noise-ratio (SNR) and low channel estimation errors. Thus, the presented system outperforms the conventional system under these conditions.

The performance of high-rate $(5/4)$ STBC and Liu rate-one (Liu *et al.*, 2002) are compared using simulation results under perfect and imperfect CSI in time-selective environment. Also, the performance evaluation of high-rate $(9/8)$ STBC and Alamouti rate-one (Alamouti, 1998) are compared under perfect and imperfect CSI in time-nonselective environment. It focuses on the adverse effects of imperfect CSI at the receiver on SER and effective throughput performances. The proposed high-rate STBC systems outperform the conventional rate-one STBC systems in the presence of Doppler spread and CFO under prevalent conditions.

**Keywords:** STBC, channel state information, Doppler spread, carrier frequency offset, autoregressive, effective throughput, flat-fading

# TABLE OF CONTENTS

# LIST OF ACRONYMS AND ABBREVIATIONS

| | |
|---|---|
| AR | Autoregressive |
| AWGN | Additive White Gaussian Noise |
| BER | Bit Error Rate |
| CDF | Cumulative Distribution Function |
| CFO | Carrier Frequency Offset |
| CSI | Channel State Information |
| CUB | Chernoff Upper Bound |
| D-STBC | Differential STBC |
| DS | Doppler Shift $f_d = f_D$ |
| EM | Expectation Maximization |
| FER | Frame Error Rate |
| ISI | Inter Symbol Interference |
| LLS | Linear Least Square |
| LOS | Line of Sight |
| LS | Least Squares |
| MATLAB | Matrix Laboratory |
| MIMO | Multi Input Multi Output |
| MISO | Multiple Input Single Output |
| ML | Maximum Likelihood |
| MMSE | Minimum Mean Squared Error |
| MRRC | Maximal Ratio Receiver Combining |
| MTAS | Multiple Transmitting Antenna Scheme |
| NVFF | Numeric Variable Forgetting Factor |
| OFDM | Orthogonal Frequency Division Multiplexing |
| O-STBC | Orthogonal Space Time Block Coding |
| PAM | Pulse Amplitude Modulation |
| PDF | Probability Density Function |
| PMPR | Peak to Minimum Power Ratio |
| PSK | Phase Shift Keying |

| | |
|---|---|
| QAM | Quadrature Amplitude Modulation |
| QO-STBC | Quasi Orthogonal Space Time Block Coding |
| QPSK | Quadrature Phase Shift Keying |
| SER | Symbol Error Rate |
| SIMO | Single Input Multiple Output |
| SNR | Signal to Noise Ratio |
| ST | Space Time |
| TRAI | Telecom Regulatory Authority of India |
| ZF | Zero Forcing |

# LIST OF FIGURES

# LIST OF TABLES

*Chapter 1*

# INTRODUCTION

*In this chapter, the concept of space-time-block-coding (STBC) and different types of fading are introduced. The objective of thesis report has also been given in this chapter.*

## 1.1 Introduction to Wireless Communication

The upcoming wireless systems are expected to have exceptional quality and coverage area and are considered to be effective in power and bandwidth requirements. Thus, the wireless communication system is needed to attain high data rate, high flexibility and to minimize the major issues related to the ongoing wireless system, one of which is multipath fading [1]. Numerous techniques that have been selected to suppress the effects of multipath fading are receiver diversity and transmitter diversity. Receiver diversity means handling multiple antennas on the receiver side and transmitter diversity means handling multiple antennas on the transmitter side. These reduce the effects of multipath propagation is the reason of multipath fading [2]. Enhancing the quality or degrading the effective error rate in the multipath system is very challenging. Prior to transmission, we need to meet a lot of challenges like modulation, encoding (channel as well as source) etc. Multipath fading may occur in any environment. The signal may take different paths from the transmitting antenna to reach the receiving antenna [3]. High-rate STBC has been employed by modifying the existing algebraic function in quasi-orthogonal STBC (QO-STBC) in the quaternion for the two transmitter antennas [4]. Diversity gain and complexity in decoding can be reduced for three and four transmit antennas by performing mathematical modifications [5]. Sometimes, when the channel is not perfectly estimated it degrades the performance of the system [6]. When the channel is time-varying in nature, its response can be expressed as an autoregressive (AR) process [7]. For a multipath fading system, the path taken by the signal may be a straight line or it may get reflected from the obstacles because of the mobility of the transmitter and receiver in the wireless communication system. The signal may completely fade out in the extreme case of fading i.e., deep fade. Thus, the strength of the signal falls beneath the usable limit. Fading generally affects the strength of the signal. Different types of fading can be analyzed with the help of Fig. 1.1. Considering small scale fading, signal

strength varies rapidly over short travel distance. Theoretically, one of the most efficient procedures to abate the effect of multipath fading involves controlling the transmitter power in a wireless communication channel. Assuming that the channel, as observed by the receiver, is already known at the transmitter side, the signal can be pre-modified by the transmitter so as to overcome the effect of the channel [1]. To overcome the minimum level of fading, the power of the signal at transmitter must be adjusted accordingly which in most of the cases, is not possible due to restrictions on the maximum signal power as well as the size and expenditure of the amplifiers [1]. Likewise, the channel observed at the receiver side is unknown therefore the transmitter needs channel knowledge to be fed back from the receiver. In some cases, feedback link may not available [1]. This results in throughput deterioration and additional complexity for both the transmitter and the receiver.

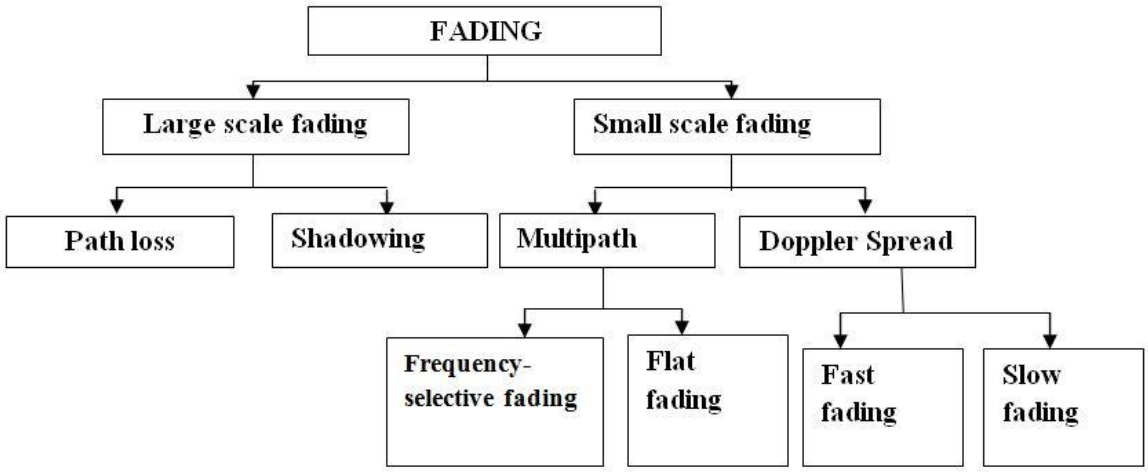


**Fig. 1.1.** Classification of fading signal [8].

In the classical technique [3], multiple antennas at the receiver combine and switch the signal such that it improves the quality of the received signal. This approach involves single-input-multiple-output (SIMO) [3]. The main drawback on employing the maximal-ratio-receiver-combining (MRRC) technique includes expensiveness, dimensions, and capability of the remote units, which will keep on growing exponentially with the growth of the emerging technologies. Thus multiple-input-single-output (MISO) and multiple-input-multiple-output (MIMO) techniques are used to neutralize the effect of multipath fading. The ease of installing multiple base stations and maintaining them at the transmitter's side also

contributes to the development of these techniques. The implementation of MIMO provides outstanding performance in terms of data rates. So, transmit diversity schemes are highly employed. Hence, MIMO and MISO schemes are preferred over SIMO technique because of their performance advantages and ease of installations. We shall investigate some terms, which are related to MIMO system in the following chapters. The basis of our study is the perfect and imperfect estimation of the channel.

## 1.2 Motivation of the Work

Recently, the demand for wireless transmission with high data-rate for multiusers and high system capacity has increased [2]. The system performance can be enhanced by employing transmitter diversity scheme because it mitigates the effects of multipath fading and thus, improves signal-to-noise-ratio (SNR) [1], [3]. This method utilizes the theory of orthogonal design for $2\times1$ STBC system and quasi-orthogonal (QO) designs for $4\times1$ STBC system, which provides high transmission rates in addition to partial diversity gain [4], [5]. Due to high-rate at improved SNR, it can accommodate more data in lesser bandwidth. In this work, the power scaling strategy in combination with space-time block-codes for $4\times1$ STBC system is used [2], [4]. Through this technique, the achievable data-rate is $5/4$ for $2\times1$ STBC system and $9/8$ for $4\times1$ STBC system. The underlying wireless channel is modeled as an AR first-order process, which is dependent on Doppler shift and carrier-frequency-offset (CFO). We report the performance results of these schemes under the imperfect channel-state-information (CSI), and compare it with perfect CSI case [6]. The CFO affecting effective throughput performance has also been analyzed. Achieving perfect CSI is not possible due to the time-varying property of the channel. Simulation results reveal that the high transmission rate is favored by high SNR and low channel estimation errors.

In the present day scenario, the requirements of communication engineering are very demanding. Considering, the prevalent communication systems, such as STBC system, the modulation is performed on the input signal. While transmitting the signal through the wireless channel, it gets affected by channel noise and additive-white-Gaussian-noise (AWGN). Thus, the strength of the received signal is degrades and thereupon the entire performance of the system declines.

These methods depend on experimentation and analytical investigation. The field test is one of the options for the experimentations in the wireless mobile environment but it is expensive and requires authorization from telecom-regulatory-authority-of-India (TRAI). Restrictions arising from the field test experimentations can be performed using a simulator.

Simulation models give us an insight to the real-world techniques. The model incorporates the key characteristics and performance/functions of the preferred physical or abstract system. In addition, simulations can also used to present the absolute effects of different circumstances. Thus, it is of utmost importance to the researchers as it deals with the real world phenomenon.

Simulators can implement evaluation of different modulation schemes. Random binary array sequences are generated and modulated using different modulation schemes such as quadrature-phase-shift-keying (QPSK), quadrature-amplitude-modulation (QAM), etc., through the simulator. Following this, the binary sequence is subjected to AWGN and channel noise in the wireless channel. Channel noise is generated due to the imperfect channel state estimation which has Rayleigh probability-density-function (PDF). The results of the simulations are plotted for symbol-error-rate (SER) and effective throughput against both SNR and channel estimation error (dB).

## 1.3 Thesis Objective

The methods discussed in this dissertation have been implemented to study the effects of channel estimation error in STBC system under Rayleigh fading distribution, considering the imperfect CSI. The research work shows that STBC system with channel noise in frequency-domain can be represented as

$$R_k = H_k S_k + N_k \tag{1.1}$$

where, $R_k$ is the received symbols vector, $S_k$ is the transmitted symbols vector, $H_k$ is the channel matrix and $N_k$ is AWGN.

It focuses on the adverse effects at the receiver, due to the imperfect CSI. The channel estimators cannot maintain perfect CSI on the receiver side. This work focuses on enhancing the data rate for two transmitting antennas and one receiving antenna under the time-selective

environment. It also focuses on increasing its effective throughput while reducing its error performance whereas, enhancement is also done for four transmitting antennas and one receiving antenna in a time-nonselective environment in terms of its effective throughput and SER.

## 1.4 Organization of Thesis

In the following chapters, discussion is done as

- **Chapter-2** discusses the literature study for imperfect channel estimation system in the time-selective and time-nonselective environment.
- **Chapter-3** gives a brief description, mathematical model, block diagram and employment of STBC system using Matrix-Laboratory (MATLAB).
- **Chapter-4** introduces various types and models of the fading environment. It studies the effect of the noise and different types of fading distribution on the signal.
- **Chapter-5** discusses the high-rate STBC communication system under Rayleigh multipath fading channel. In this work, we have evaluated the performance under two conditions. Former is perfect CSI and latter is imperfect CSI.
- **Chapter-6** gives the conclusion of our work and future scope is also suggested.

*Chapter 2*

# LITERATURE REVIEW

*In this chapter, a brief introduction about detrimental effects of channel estimation errors is given. The techniques available in literature work discuss performance of STBC systems in time-selective as well as frequency-selective environment under both perfect and imperfect channel estimation scenarios.*

---

In [1], Alamouti has proposed a new symbol transmission scheme with two transmit antennas known as orthogonal-STBC (O-STBC), in which coding of symbols is done in both space and time-domains. It attains the same diversity scheme as achieved by maximal-ratio-receiver-combining (MRRC). This new scheme can be generalized to more than one receiver antenna to achieve full rate (rate-one). In this new scheme, feedback path is not needed from the receiver to the transmitter antenna for the bandwidth expansion and on calculation, author attained that its complexity is similar to MRRC. This novel transmit diversity advent can be realized to enhance the information rate, error realization, and scope in the wireless communication system. Here, the reduced susceptibility to the fading can authorize the usage of higher-order modulation patterns in increasing the effective information rate.

In [2], Das *et al.* have introduced an innovative technique for rate-5/4 O-STBC with full-diversity. It is introduced by extending the signal set from the quaternions pre-owned in the Alamouti technique. QPSK modulation with two transmitting antennas is used. Discriminative power scaling of message symbols has been utilized to guarantee full-diversity. Here, the coding gain has been maximized in addition to the minimizing the transmitted signal peak-to-minimum power scale. The mathematical derivation of the power-scaling technique is done and it has been proved that this scheme supersedes the constellation rotation based scheme with a low-complicated decoder working on ML technique through which decision can be made in the favor of transmitted symbol. It has been shown that the increase in the information rate is 25% more than the conventional data rate. The two techniques can be used in switchable manner to increase the throughput at all the SNR values. This work discusses the power-scaling which results in better throughput level than the

constellation rotation scheme. In the end, the designs have been extended to 4 transmit antennas, thus extending the set of QO-STBC by considering the power-scaling.

In [3], Jafarkhani has proposed an innovative approach for communication using various transmitting antennas under Rayleigh and Rician fading channels. The codes are linearly processed using maximum-likelihood (ML) decoding for random real constellations pulse-amplitude-modulation (PAM). Designing of STBC has been done that such attains the highest possible transmission rate for N transmitter antennas. For three or four transmit antennas rate-one code cannot be attained but for rate $3/4$ codes, full diversity can be attained. In general, for any count of transmitting antennas maximum obtainable transmission rate is $1/2$.

In [4], Grover and Kohli have discussed numeric-variable-forgetting-factor (NVFF) combined with least-square (LS) algorithm to estimate the channel. The technique is modulated with QPSK digital modulation technique. The frame-error-rate (FER) of full-diversity high-rate STBC system is presented. This technique allows full-diversity for two transmitter antennas and partial-diversity for four transmitter antennas. High data rates of $5/4$ for two transmit antennas and $9/8$ for four transmitter antennas can be obtained for a STBC system. It is accomplished by augmenting the coding gain combined with reduced peak-to-minimum-power-ratio (PMPR). Selective power scaling is used on the data symbols. The scaling factor is taken to be greater than one and is separately derived analytically for $2\times1$ and $4\times1$ antenna systems. The power scaling factor is integrated with the constellation rotation schemes. With this, authors can switch between the two constellations with two different radii. Power scaling occurs in inner constellation circle. Deterioration of the FER performance is observed, when the channel is imperfectly estimated employing low complex ML decoding algorithms. The simulation results shows that the performance of FER employed for high-rate STBC system under ideal channel estimation conditions differs from its performance when used with real wireless scenario because of the effects of the errors in the channel estimation. Here, the technique is extended to general M-ary PSK constellations. The linear-least-square (LLS) algorithm employing NVFF is used as pilot symbols performing as channel estimator. The tracking performance of pilot channel estimation has been observed to be an important part of the presented wireless system, when working in slow time-varying channels. This scheme can be further extended to eight transmitter

antennas and can be used in collaboration with OFDM technique for further enhancement of the data rates.

In [7], Liu *et al.* have proposed an innovative decoding technique for Alamouti's STBC transmissions done using time-selective Rayleigh multipath fading mediums. The time-selective channels have been designed as a random process. Kalman filter provides channel tracking of these time-selective channels, thereby, enabling the decoding using space-time (ST) decoding. In this work, the channel has been projected as an AR process which includes channel variations depends on Doppler variation and local oscillator frequency mismatch between transmitter and receiver, which is denoted by CFO.

In [11], Su and Xia have discussed channel estimation with data distribution detection considering multiple radio channels having numerous transmitter and receiver antennas. Here, expectation-maximization (EM) algorithm has been implemented on the receiver antennas. Performance has been examined on the Rayleigh fading multipath channel. Iterations at the receiver can be expressed by two steps: minimum-mean-squared-error (MMSE) is calculated which gives the antecedent measure of the data. It is later detected using Viterbi algorithm.

In [12], Zhuang has made the assumption of the availability of the CSI on the receiver side. In addition to this, the partial channel information is also fedback to the transmitter side. Here, the detailed realization of bit-error-rate (BER) performance of multiple-transmitting-antenna-scheme (MTAS) for the STBC system with MISO system has been studied. Simultaneously, the drafted paradigm for MISO-STBC system, which maximizes the channel Frobenius norm and reducing the error probability has been used. Here, the mathematical expressions and model of the wireless channel for both imperfect CSI case and perfect CSI case have been examined. Consequently, the case of perfect CSI evaluation on the BER execution of the Chernoff-upper-bound (CUB) with adequate complexity and multiple transmitting antenna preference system are assessed for the MISO-STBC system. Extension to the former technique, an extensive mathematical interpretation of BER-CUB for the same system has also been derived. Finally, the mathematical study of this work has been verified and supported by exhaustive Monte-Carlo simulations. MTAS is capable of minimizing the outcomes of the erroneous CSI which is demonstrated by the simulation results and also with the mathematical results.

In [13], Tarokh *et al.* have designed channel codes for multiple transmitting antennas in order to enhance the data rate as well as to increase the reliability of the communication system working under fading channels. Encoding of the data has been done by the channel coder, thus the data which is to be encoded, is split into N paths, which are then synchronously communicated when using N transmitter antennas. Each receiving antenna performs the summation of the N transmitted signals which is affected by noise. The performance criterion has been derived for these codes considering the supposition that the fading must be slow and frequency-nonselective. Performance is decided with the matrices formulated against the combination of noticeable code sequences. Diversity gain is measured by the minimal rank amidst these matrices, whereas coding gain is measured by the minimum determinant of the matrices. The outcomes are thus extended to the fast fading channels. Trellis codes have been designed for high-rate wireless communication systems. These codes contribute for the perfect agreement amidst data rate, diversity improvement, and trellis complexity. Here, the simulation results are computed using 4- and 8-ary PSK signals having the data rates of 2 or 3 bits/symbol, describing the exquisite performance, which limits its outage capacity within 2–3 dB for the above channels, which needs encoders with 64 states only.

In [15], Gappmair and Bergmann have estimated channel and carrier parameters with the help of pilot-aided transmission and applying some former techniques utilizing an algorithmic procedure, which mainly focuses on analytical considerations. Here the assumption made is that the channel model can be modestly represented with respect to the correlated Rician distribution considering insignificant multiple passages and shadowing results for a ground-to-mobile satellite link. The results have been reviewed by the authors in distinction to ML trace. The ML mechanism is based on three simple steps. First, it deals with optimizing and estimating both the frequency and phase. Secondly, the Doppler spread is evaluated and finally, the signal interference with the noise power is calculated by direct averaging method in both time and frequency-domain. Bandlimited Rician fading is considered to be spectrally flat. On the basis of the above condition, the vital output of the study denotes that the ML solution is the basis of achieving the ad-hoc framework.

In [16], Diggavi *et al.* have introduced two space-time transmission techniques, which permits full-rate and full-diversity non-coherent communication and uses two transmit antennas over frequency-selective fading channels. Here, the first scheme works in the frequency-domain, where the combination is performed with differential STBC (D-STBC)

scheme with orthogonal-frequency-division-multiplexing (OFDM) technique. The second technique works in time-domain and it engages with differential time-reversal STBC to ensure blind channel identification without using multiple receiver antennas. Identification of finite-impulse-response (FIR) channels based on second-order statistics can only be done when multiple receiving antennas are used. In the first method, using D-STBC identification of the channel is enabled based on the second-order stats on a single receiving antenna and space encoding data. Thus, the two techniques used here are based on D-STBC combined with OFDM technique utilizing transmitting diversity technique to be used over frequency-selective method. The second technique involves time-domain D-STBC technique which enables channel identification on using single receiver antenna and eliminating oversampling.

In [19], Kohli has substituted the practice for featuring the time-varying flat-fading channels, which integrates the diverse ring of scatterers for the antenna array receivers around the mobile transmitter to reduce the widening of azimuth. There is a continual change in the ring-type cluster of scatterers, when the mobile unit moves. Working with the time-varying environment, correlation of the scatterers with the prior phase of the ring is performed in subsequent phases of the ring on applying the second-order Markov model. The proposed criterion calculates the interdependence of the fading waveforms and thus, it is related with the conventional systematic correlation. It is evident that the simulation results are persistent with the Jakes' model [9]. It is said to be in accordance with the current channel model being adaptable with the conventional adaptive algorithms, which are been utilized in estimating and detecting the unsteady wireless scheme.

In [21], Foschini and Gans have discussed parallel interference cancellation scheme based detectors for three and four transmitter antennas. Here, the time-selective fading channel is considered over conventional O-STBC detectors which may undergo a considerable error reduction in high SNR cases as compared to conventional O-STBC. Generally, conventional O-STBC channel remains immobile over the full length of codeword. Here, an alternative approach to the zero-forcing (ZF) detector has been proposed. This technique uses a multi-element array and it can be seen that the capacity increases when SNR increases.

In [34], Ma and Giannakis have described that many existing STBC systems consider time invariant multipath fading channels and offer full diversity gains when the channel is accurately estimated at the receiver. Authors have derived double D-STBC technique for

time-selective multipath fading channels, applicable to a random count of transmitting and receiving antennas without having any knowledge of CSI. This technique was effective in providing diversity gain when unknown frequency offsets were present. Space-time codes were drafted to reduce the BER.

In [40], Ramaswamy *et al.* have considered STBC-MIMO system in analytical form and its performance has been studied by varying the number of transmit antennas, channels, the number of receiving antennas, modulations, and their rates with the help of simulation. At every phase, different encoding matrices have been implemented. In estimation, if the channel matrix is found to be in correlation, the number of unknown variables in the equations can be greater than the number of equations and thus it becomes tough to solve for the variables mathematically. This correlation, in $H$ matrix, is the result of the spacing between antennas. The separation between antennas needs to be adjusted to discard the effects of correlation. In this case, the disadvantages of using more transmitting antennas state is that the power per transmit antenna scales down.

In [41], Zheng and Burr have considered the time-selective fast fading channel, which exists in the realistic environment due to which non-orthogonal STBC detector undergoes degradation due to high error in the performance. Here, the simple zero-forcing (ZF) detector has been implemented, which is highly efficient in combating with the effects of channel variations on the system output. It allows effective performance results in comparison to quasi-static slow fading channel based detectors. Considering slow as well as fast fading channels, the proposed detector is able to manage both continuous as well as a constant decoder.

In [43], Zheng and Burr have discussed a case of the non-quasi immobile environment, which implies time-selective, but fast fading channels. This exists in a realistic environment, where this STBC detector faces an irreducible error. Here, ZF based signal detector has been implemented, which is calculated by a simple method, but it is very efficient in reducing the effects of the channel variation on the system performance. It also allows us the system to attain the same performance as in the case of quasi-static channel decoders. Due to switching between slow fading channel and fast fading channel, diversity loss occurs. ZF detector may detect all these changes efficiently. This technique may detect symbol-by-symbol using pilot channel estimation.

In [44], Kumar and Kohli have discussed the performance of high-rate STBC schemes in frequency-selective fading environment. Inter-symbol-interference (ISI) occurs because of a large channel delay spread in the frequency-selective channel whereas in high-rate STBC, ISI occurs due to the loss of quasi-static assumption. Here, low complexity zero forcing equalizer helps in mitigating the effects of ISI by introducing the channel estimated by the equalizer and, thus, analytically reducing the diagonal elements of $H^H H$ to zero. The assumption made is that the CSI is perfectly known to the receiver. All the simulations have been performed under Nakagami-m fading channel. The frequency flat condition refers to equations that remain constant even if some quantities are allowed to vary slowly with time.

## Summary

Taking the reference of the above mentioned bibliography, this dissertation is an attempt to study the effects of channel estimation error in STBC system under the consequence of Rayleigh fading distribution, under an imperfect CSI. In the next chapter, a brief preface about the STBC system is discussed and implementation of the same has been using MATLAB.

*Chapter 3*

# BASIC SPACE-TIME BLOCK-CODING SYSTEM

*This chapter presents a brief preface about the STBC system. The discussion of the block diagram, a mathematical representation of the STBC system has been done. Here, we have reviewed STBC system by implementing it and performing simulation using MATLAB conducive to understand the performance of rate-one S. M. Alamouti system [1] and high-rate system [2].*

## 3.1 Preface

Present day MIMO technology has received adequate consideration due to the prompt development of broadband wireless communication systems for broadband applications engaging multi-transmitting and receiving antennas. For MIMO systems, theoretic results reveal that it can offer convincing capacity gains when compared to traditional single-input and single-output (SISO) channels. In current communication scenario, it has become a need to elevate the data rates so that the information is transmitted precisely and swiftly through wireless environment. Researchers have developed suitable techniques such as STBC, SFBC, etc. considering high data rate need for wireless applications.

## 3.2 Theoretical Concepts of STBC

### 3.2.1 Defining STBC

STBC has been extensively utilized by MIMO systems, as it allows transmission of various replicas of the information stream. It uses multiple antennas at the transmitter side which help in the reliable reception of all the expected forms of information, thus, resulting in higher reliability of information transfer. Received signal similarity is grouped by the STBC technique in an excellent method, such that it gets maximum information from all of the received signals. Both dimensional and temporal diversities are used by STBC.

In STBC, various replicas of information transmission exist. This removes all the effects of the channel which includes fading as well as thermal noise. Even if there is a severe

fading, reception of the information symbols replicas may be possible with less distortion at the receiver.

The encryption of the data streams is done in groups prior to the transmission when using STBC. The distribution of the information blocks is, thus, done across the multiple antennas, spaced at some distance to separate the transmission spatially; in addition spacing of data is also done with time.

An STBC system is generally represented with the help of a matrix. Time slots are represented by rows and antenna's transmission over time is represented by each column. Encoding matrix for space-time block codes is designed as follows

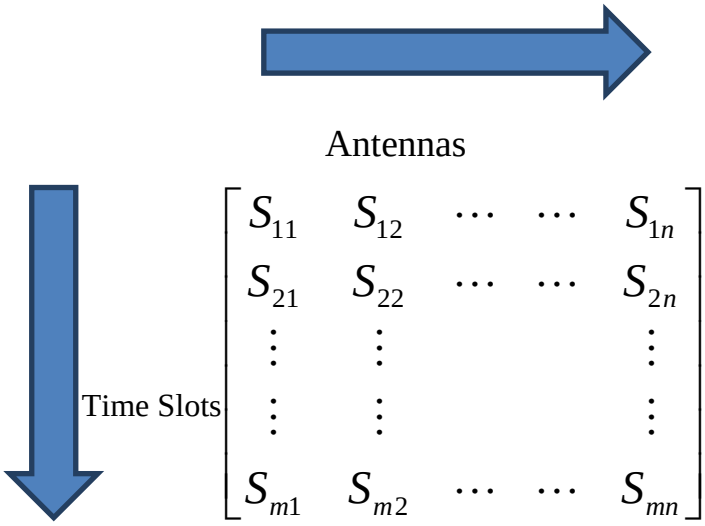


**Fig. 3.1.** STBC encoding matrix [18].

Consider the matrix represented above, in which, $S_{mn}$ represents the modulated symbol whose transmission is done in time slot $m$ from antenna $n$. T time slots exist with $nT$ transmitting antennas in addition to $nM_R$ receiving antennas. The block shown in Fig. 3.1 can be generally taken to be of length T.

Here, the data is transmitted in a number of time slots through different antennas, hence the transmission rate can be given as

$$c = \frac{s}{T} \tag{3.1}$$

where, $s$ represents the number of information symbols transmitted and $T$ the time slots.

### 3.2.2 STBC Message

STBC message is generated by encoding data in space and time. Every symbol is modulated using modulation schemes like different PSK techniques or with QAM. In this work uppercase variables are used for matrix or vector denotations and lower case variables are single matrix or vector. Modulated symbols are transmitted using STBC coding matrix in wireless channel as shown

$$R = HS + \mathrm{N} \tag{3.2}$$

where, $R$ represents the received symbol vector, H is the channel matrix, $S$ represents the modulated symbol vector and N is the AWGN vector.

In practice, the baseband STBC receiver performs the inverse of the functions which are performed at the transmitter side.

## 3.3 Mathematical Model of STBC

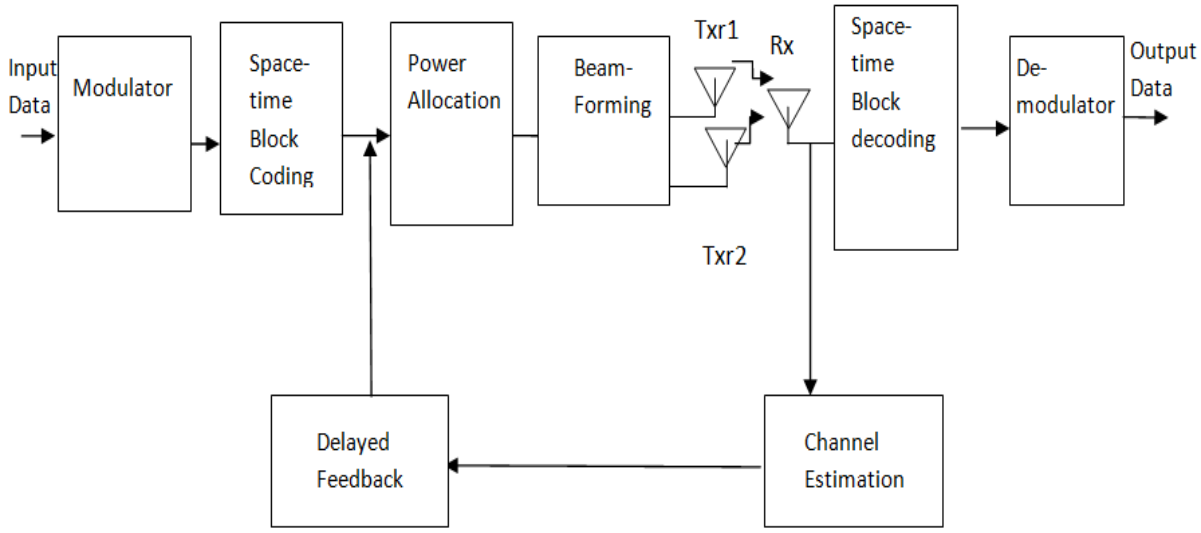


**Fig. 3.2.** Block diagram of STBC communication system [22].

In STBC system, the components on the transmitter side are an information source, modulation block along with space-time encoding matrix block whereas on the receiver side, there is space-time decoding block followed by demodulation block and thus output data is

recovered. These blocks distinguishes the function of the STBC system. In Fig. 3.2 the block schematic of an STBC communication system is shown [1]. Each of the block is then discussed separately in the subsequent part of this chapter.

### 3.3.1 Modulator

A modulator makes it possible for the wireless channel to transmit the data to a longer distance. In the modulation process, one of the parameters of the information symbol is varied with respect to a high frequency carrier signal. It helps in reducing the antenna height and these techniques can be analog or digital based on the type of message and carrier signal. Multiplexing is also possible with modulation, which involves sending multiple data on a single communication channel.

Different types of modulation techniques are shown in Fig. 3.3.

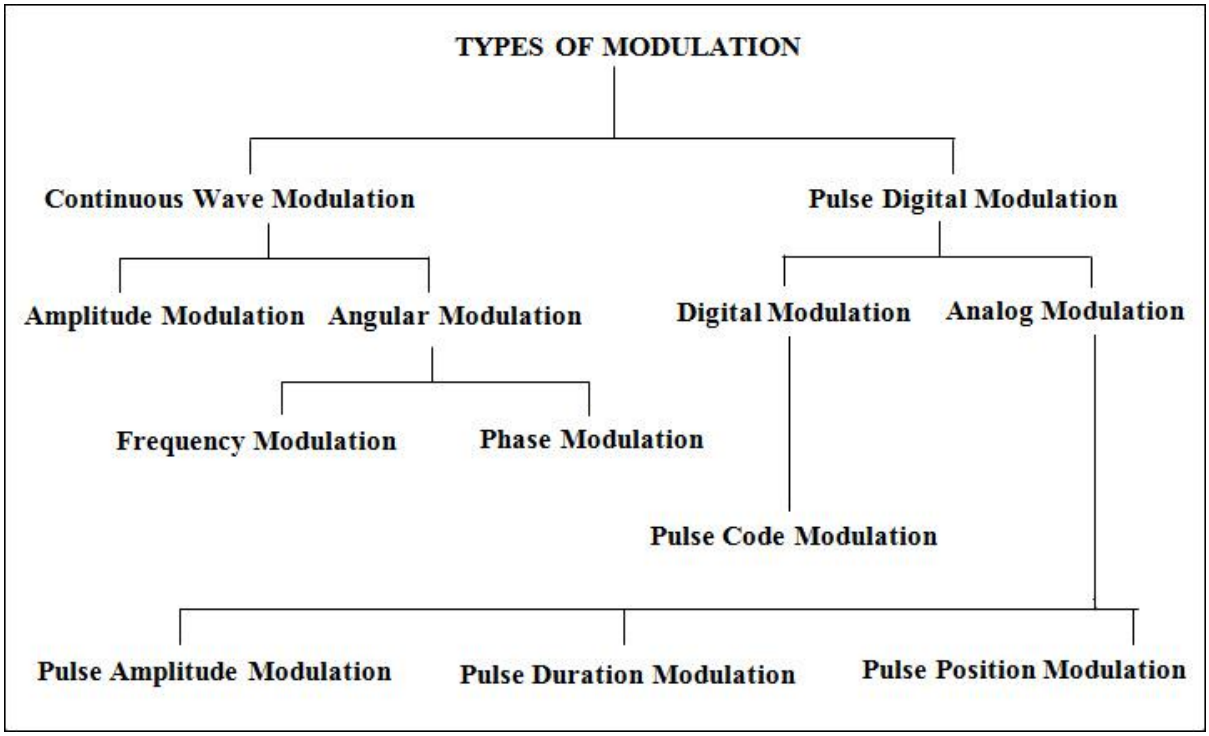


**Fig. 3.3.** Different types of modulation techniques [26].

### 3.3.2 Space-Time Coding

Space-time coding is employed using multiple transmitter antennas and achieving temporal as well as spatial redundancy from the data, which is achieved by antenna arrays. In space-

time coding, two fundamental aspects are possible. The first aspect is based on the fact that the receiver has the prior knowledge of the channel experienced by the information symbols. Hence, the data can be coded and sent accordingly whereas in the second aspect, only fixed codes can be used for different data rates. In this approach, transmitted power is shared by all the transmitters equally. Two important categories of space-time codes described as

- Block orthogonal codes
- Space-time trellis codes

### 3.3.3 Power Allocation

Achieving adaptive power allocation in wireless communication leads to the increase in capacity. Specifically, this capacity is termed as ergodic capacity. The three major power limitations are

- Battery life of mobile.
- Power level assigned to the device by the government bodies or due to interference causes.
- Each transmitter antenna range is different and thus difficult to design practical designs for each antenna individually.

### 3.3.4 Beamforming

Beamforming is used to achieve required directive pattern for any set of antennas. It is used to achieve the mandatory performance level of any system and is used for smart antennas. In phased array systems, the knowledge of the path of a pre-defined signal should be achieved. According to the pre-defined beam, direction switching of the beam should be done in a suitable direction. In this technique, the required direction and the fixed beam should be determined.

For moving systems, we cannot rely on the fixed beam system, therefore, the beam is directed to an infinite number of patterns and should be adjusted according to the real-time. For moving objects, adaptive array beamforming is used. This system is more expensive and complex.

### 3.3.5 Transmission

The transmitter is used to convert the information symbols into a specific required form. On the transmitter side, various techniques are performed, which are already explained above. In this process, the data is transmitted through a wireless channel through two different antennas.

### 3.3.6 Receiver

The receiver receives the data, which has been transferred through the wireless link. During this transfer some of the data gets corrupted by the channel noise as AWGN. The data is received in the same form as it was transmitted i.e., in its original form with some errors. At the receiver side, exactly opposite process is followed as is done at the transmitter side.

### 3.3.7 Space-Time Block Decoding

STBC decoding is done using maximum likelihood decoding. Decoding of the signal is done symbol by symbol and not as a whole. Due to this, ML scheme finds the minimum distance between the transmitted symbol and received symbol. Thus the decision can be made between the transmitted symbols.

### 3.3.8 Demodulator

Demodulator separates the original data from the modulated data removing the carrier signal as shown in Fig 3.4. It performs the exact reverse process done at transmitter's side. The demodulated signal is a low-frequency signal.

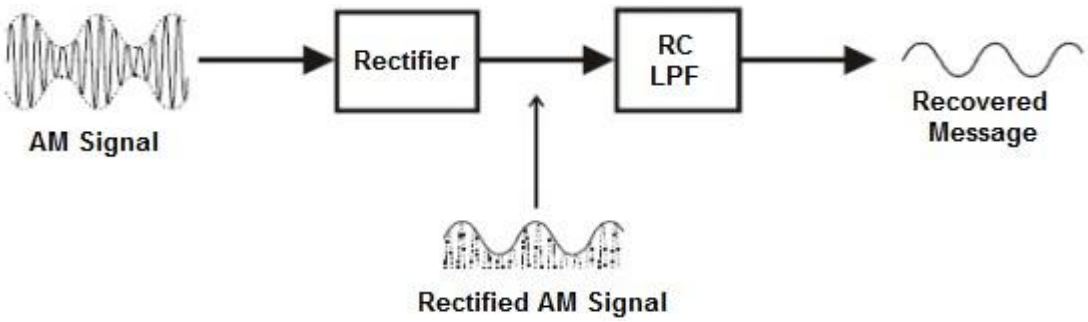


**Fig. 3.4**. Demodulation of an AM signal [26].

### 3.3.9 Delayed Feedback

The feedback delay affects the channel estimation in a MIMO system. It also affects the outage capacity of the system. As the SNR is increased, feedback delay results in deterioration of the system performance. Channel prediction is done with the help of feedback but it results in degradation of system performance.

### 3.3.10 Channel Estimation

Channel estimation includes two further divisions. They are mentioned below

- *Channel information known at both transmitter and receiver*- In this technique, the transmitter can precode the signal and transmit it. With the help of this, all the distortions going on in the channel is known and with this, the required transformations can be made, so as to make an efficient transmission of the signal.
- *Channel information unknown at receiver*- In this, no feedback is given to transmitter, and thus the received data has some channel estimation errors associated with it. Here, no precoding of the data can be done prior to the transmission. It results in declining the performance as compared to the former technique.

## 3.4 Design Criterion

In our system, the input is applied in a complex vector form which is modulated with the QPSK or QAM digital modulation technique. The input vector is $S = \left[S_0\ S_1\ S_2 \ldots S_{N-1}\right]^T$, where N is the vector length. Space-time encoding is performed for the input $S$ based on the Eq. (3.2)

Mostly, PSK modulation is used in STBC systems, thus, each of the elements of $S$ can be represented as a PSK constellation point. The output is in the form of a digital complex vector for a space-time encoder ($s = [\mathrm{s}_0\ \mathrm{s}_1 \ldots\ldots\ldots\ldots \mathrm{s}_{N-1}]^T$) and, thus, it is fed to the space-time decoder block after wireless transmission through the channel.

Fig. 3.5 represents the basic schematic representation of the Alamouti scheme. The input is applied in vector form to the modulator block in the form of random variable for 4-PSK constellation which are represented as $\{1+j, 1-j, -1-j, -1+j\}$. Encoded data transmitted

through a wireless channel, gets corrupted by channel noise. Hence, to calculate BER the received signal, after space time decoding, is demodulated and compared with the transmitted signal. The BER is then plotted against SNR.

### 3.4.1 Conventional STBC Scheme

- **Alamouti Space-Time Block-Code**

A two-branch simple transmit diversity technique is proposed by Alamouti [1]. This scheme provides same diversity order comprising of two transmitting antennas and one receiving antenna, as compared to the MRRC utilizing one transmitting antenna and two receiving antennas. It has been shown here that further advancement can be done in this scheme easily by extending it to two transmitter antennas and $M_R$ receiver antennas, which provides the diversity order of $2\times M_R$. Thus, the novel technique does not need any increase in the bandwidth and feedback path from the receiving antenna to the transmitting antenna, and also its computational complexity is comparable to that of MRRC.

Encoding matrix for Alamouti scheme is given as

$$G=\begin{bmatrix} s_o & s_1 \\ -s_1^* & s_o^* \end{bmatrix} \tag{3.3}$$

where, $s_o, s_1$ represents the space-time transmitted symbols and $(.)^*$ denotes the conjugate operator. The channel, as experienced by the transmitting and the receiving antenna zero represented by $h_0$ and the channel experienced by the transmitting and receiving antenna one represented by $h_1$ where,

$$h_o = a_o \exp(j\theta_o) \tag{3.4}$$

$$h_1 = a_1 \exp(j\theta_1) \tag{3.5}$$

where, $a_o$ and $a_1$ represents the magnitude response of the channel and $\theta_o$ and $\theta_1$ represents the phase response of the channel. The noise along with interference is summed together on the two receiving antennas. The result of the above process shown in the form of baseband signal is shown as

$$r_o = h_o s_o + \eta_o \tag{3.6}$$

$$r_1 = h_1 s_1 + \eta_1 \tag{3.7}$$

It is assumed that $\eta_0$ and $\eta_1$ is Gaussian distributed. The ML decoding is done on the receiver to ensure about the decision for choosing $s_i$ if and only if

$$d^2\left(r_o, h_o s_i\right) + d^2\left(r_1, h_1 s_i\right) \leq d^2\left(r_o, h_o s_j\right) + d^2\left(r_1, h_1 s_j\right) \forall \ \mathrm{i} \neq j \tag{3.8}$$

where, $d^2$ represents the square of the Euclidean distance calculated between signals $p$ and $q$ using the mathematical formula as in [1].

$$d^2\left(p, q\right) = \left(p - q\right)\left(p^* - q^*\right) \tag{3.9}$$

The receiver diversity scheme representing two-branch MRRC is shown as

$$s_o = h_o^* r_o + h_1^* r_1 = (\alpha_o{}^2 + \alpha_1{}^2)\mathrm{s}_o + h_o^* \eta_o + h_1^* \eta_1 \tag{3.10}$$

After using above equation, we get the estimated equations as

$$s_o = (\alpha_o^2 + \alpha_1^2)\left|s_i\right|^2 - \tilde{s}_o s_i^* - \tilde{s}_o^* s_i \leq (\alpha_o^2 + \alpha_1^2)\left|s_j\right|^2 - \tilde{s}_o s_j^* - \tilde{s}_o^* s_j \ \forall \ \mathrm{i} \neq j \tag{3.11}$$

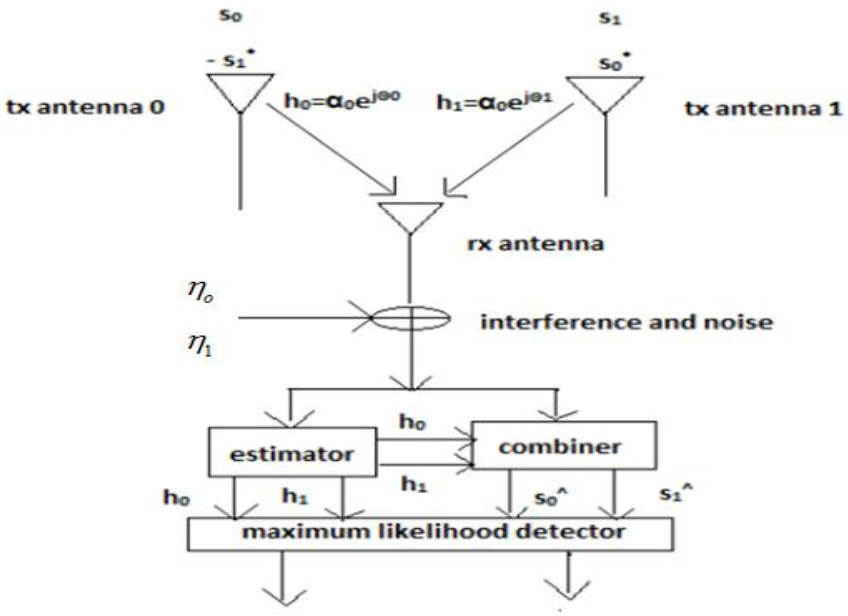


**Fig. 3.5.** Representation of an Alamouti scheme [1].

### 3.4.2 Time-Selective STBC Scheme

Considering Alamouti coding where the channels are assumed to be flat whereas for this technique time-selective but frequency-flat channels have been acknowledged [7]. In the time-selective environment, $h_i(k), i=1,2$ denotes the channel coefficient from the $i^{th}$ transmitting antenna to the receiving antenna. The two consecutive received samples have been shown [7] by Eq. (3.13) and Eq. (3.14)

$$R(2k) = \mathrm{h}_1(2k)\mathrm{s}(2k) + \mathrm{h}_2(2k)\mathrm{s}(2k+1) + \eta(2k) \tag{3.12}$$

$$R(2k+1) = -\mathrm{h}_1(2k+1)\mathrm{s}^*(2k+1) + \mathrm{h}_2(2k+1)\mathrm{s}^*(2k) + \eta(2k+1) \tag{3.13}$$

where, $\eta(k)$ represents the noise as the complex Gaussian random variable.

Since, this model is AR, so $h_i(k)$ varies [7] as in

$$h_i(k) = \alpha h_i(k-1) + v_i(k) \tag{3.14}$$

where, $v_i$ is zero-mean complex Gaussian noise and the coefficient α can be determined by

$$\alpha = E\left[h_i(k)h_i^*(k-1)\right] \tag{3.15}$$

where, $E(.)$ denotes expectation operator[10].

Wireless channel deviations can primarily occur due to two independent sources. Firstly, the Doppler effect which originates due to the relative motion between the transmitter and the receiver. Secondly, the CFO which occurs due to the transmitter–receiver oscillator's mismatch. The CFO is denoted by $f_o$ and the information symbol duration by $T_s$. Consequently, we can factorize $h_i(k)$ into

$$h_i(k) = \overline{h_i}(k)\exp\left(j2\pi f_o T_s k\right) \tag{3.16}$$

where, $\overline{h_i}(k)$ accounts for Doppler shifts, but according to Jakes' model [9], we have

$$E\left[\overline{h_i}(k)\overline{h_i}^{*}(k-1)\right] = J_o(2\pi f_d T_s) \tag{3.17}$$

where, $J_o(.)$ is the Bessel function of zeroth-order and first-kind and Doppler shift is denoted by $f_D$, thus $\alpha$ is related to the $f_D = f_d$ and $f_o$ as

$$\alpha = J_o(2\pi f_d T_s)\exp(j2\pi f_o T_s) \tag{3.18}$$

Now we proceed with the space-time decoding with respect to different values of $\alpha$. The only difference is channel response being autoregressive and the effect of feedback.

Decoding is done as follows

$$R(k) = H(k)S(k) + \mathrm{N}(k) \tag{3.19}$$

where, $\mathrm{R}(k) = \left[r(2k), \mathrm{r}^{*}(2k+1)\right]^{T}$, $\mathrm{N}(k) = \left[\eta(2k), \eta^{*}(2k+1)\right]^{T}$ and

$S(k) = \left[s(2k), \mathrm{s}(2k+1)\right]^{T}$ and the channel matrix is defined as

$$H(k) = \begin{bmatrix} h_1(2k) & h_2(2k) \\ h_2^{*}(2k+1) & -h_1^{*}(2k+1) \end{bmatrix} \tag{3.20}$$

To decode $S(k)$ from $Y(k)$, we form the decision vector $\mathrm{Z}(k) = \left[z(2k), \mathrm{z}(2k+1)\right]^{T}$

$$Z(k) = H^{H}(k)R(k) \tag{3.21}$$

Multichannel estimation task becomes challenging mainly in the time-varying MISO system. Favorably, the AR model can be used to track the variation in the channel using Kalman filtering.

### 3.4.3 High-Rate STBC Scheme

In this work, the objective is to improve a novel class full diversity high-rate system [2]. The transmission rate is generally greater than 1 by utilizing the basic algebraic arrangement in already existing orthogonal designs stationed on the quaternion for two transmitter antennas

[1]. Quasi-orthogonal designs are used for four transmit antennas [3]. The representation of a complex orthogonal design for $2\times 2$ code is given as

$$Q(s_1, s_2) = \begin{bmatrix} s_1 & s_2 \\ -s_2^* & s_1^* \end{bmatrix} \tag{3.22}$$

The accord between Alamouti matrices and quaternions shows that specified Alamouti matrices are developed using addition, multiplication, and inversion. Coset of Eq. (3.23) is given as

$$\bar{Q}(s_1, s_2) = \begin{bmatrix} s_1 & s_2 \\ s_2^* & -s_1^* \end{bmatrix} = \begin{bmatrix} 1 & 0 \\ 0 & -1 \end{bmatrix} Q(s_1, s_2) \tag{3.23}$$

In the novel technique, the space-time signaling matrix transmission has been chosen from either *Q* or its coset $\bar{Q}$. The selection is based on supplementary information bit 0 or 1 mapped to *Q* or its coset respectively. Hence, the novel technique attains a 25% increase in the information rate, when compared to the traditional Alamouti scheme employed for *QPSK* modulation, without needing any supplementary system resources.

The output symbols received vector matrix after decoding over two consecutive symbol periods are expressed as

$$\begin{bmatrix} r_1 & r_2 \\ -r_2^* & r_1^* \end{bmatrix} = \begin{bmatrix} h_1 & h_2 \\ -h_2^* & h_1^* \end{bmatrix} \begin{bmatrix} s_1 & s_2 \\ -s_2^* & s_1^* \end{bmatrix} + \begin{bmatrix} \eta_1 & \eta_2 \\ -\eta_2^* & \eta_1^* \end{bmatrix} \tag{3.24}$$

where, $R = \begin{bmatrix} r_1 & r_2 \\ -r_2^* & r_1^* \end{bmatrix}$ and $H = \begin{bmatrix} h_1 & h_2 \\ -h_2^* & h_1^* \end{bmatrix}$

and

$$\begin{bmatrix} r_1 & r_2 \\ r_2^* & -r_1^* \end{bmatrix} = \begin{bmatrix} h_1 & h_2 \\ -h_2^* & h_1^* \end{bmatrix} \begin{bmatrix} s_1 / \mathrm{p} & s_2 / p \\ s_2^* / p & -s_1^* / p \end{bmatrix} + \begin{bmatrix} \eta_1 & \eta_2 \\ \eta_2^* & -\eta_1^* \end{bmatrix} \tag{3.25}$$

where, $\bar{R} = \begin{bmatrix} r_1 & r_2 \\ r_2^* & -r_1^* \end{bmatrix}$

Here, $R$ and $\bar{R}$ is the received vector matrix depending on the transmitted symbol matrix on the basis of quaternions. $h_1, h_2$ denotes path gains of the channel matrix and $\eta_1, \eta_2$ denotes the noise vector. After matched filtering operation, we can decode received symbols and compare the decoded symbols with the transmitted symbols.

### 3.5 Simulation Results for Conventional STBC System

STBC based simulator uses BPSK/QPSK modulation techniques to find the variation in BER/SER for different SNR. Table 3.1 depicts all parameters used in simulation for the STBC system.

| Parameter | Value |
|---|---|
| Modulation used | BPSK, QPSK |
| SNR(dB) | 0 to 15 |
| MRRC scheme | $1\times 2$ |
| Alamouti scheme | $2\times 1$ |
| Channel | Rayleigh |

**Table 3.1.** STBC system parameters used for simulation.

- **Alamouti Compared with MRRC**

In this work, we have plotted the BER performance of BPSK for MRRC and the new transmitter diversity scheme, i.e., Alamouti scheme considering Rayleigh fading environment. The assumption made is that from the two transmitting antennas, total transmitted power for the Alamouti technique is same as the transmitting power for the single transmitting antenna in MRRC. Another assumption made is that the amplitudes of fading from every transmitting antenna to corresponding receiving antenna are considered to be jointly uncorrelated Rayleigh distributed. The average signal strength at the receiving antennas compared with each transmit antennas are alike. Additional assumption made here is that the receiver to have the perfect CSI. All the assumptions, despite being impractical in the real world scenario, provide a reference to the performance curves when compared with other simulations.

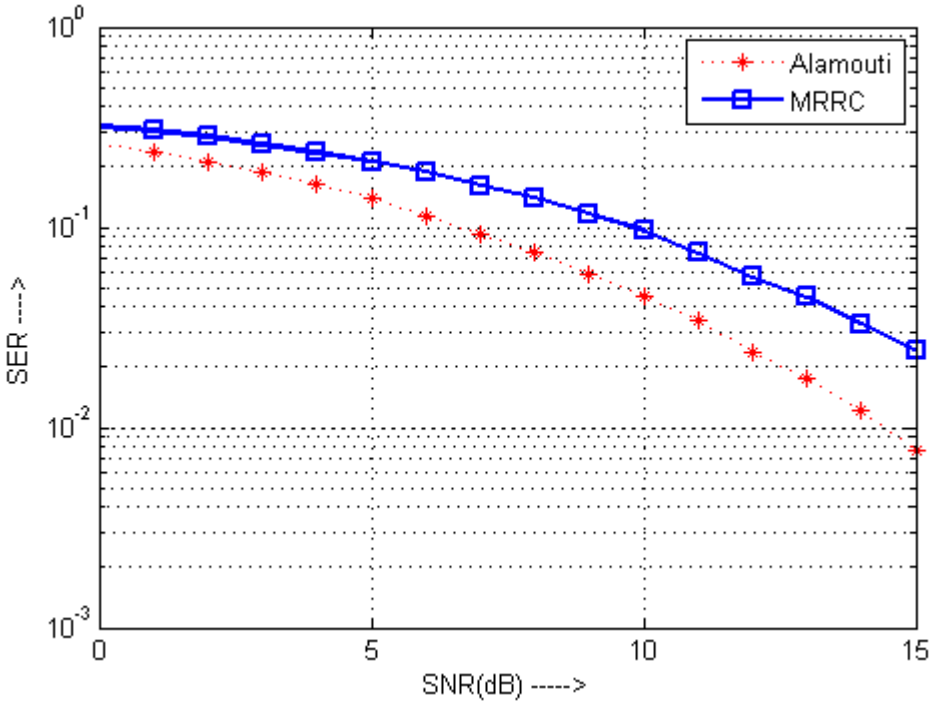


**Fig. 3.6.** Simulation results of an Alamouti scheme vs. MRRC [1].

It can be concluded here that the novel scheme [1] is providing the identical performance when compared to MRRC. Here the selected coding, as well as the modulation techniques does not affect the performance similarity of the new scheme with the conventional one. A lot of publications have shown the effect on the performance using different coding and modulation schemes employed with MRRC. On the basis of results studied from the above techniques, further prediction of the results can be done in a different environment.

## 3.6 Benefits of STBC System

The main benefits of STBC system are

1. MIMO-STBC system is relatively fast and is more robust system.
2. It provides increased capacity when compared to the SISO system.
3. STBC system is reliable to the failure of any path because if one path fails, the data can be received through the other path.
4. It provides protection against interference when used in conjunction with the array processing techniques.
5. By using pilot symbols we can estimate channel more effectively.

## 3.7 Limitations of STBC System

The main limitations of STBC are

1. The coding and decoding is relatively complex.
2. The mismatching of the local oscillator at both of the transmitter and receiver sides, leads to CFO which causes time variation in the signal.
3. Frequency offset errors are caused by Doppler shifts, i.e., when either transmitter or receiver or both are in motion thus causing data disruptions.
4. STBC system provides 3dB penalty in the BER performance when compared to MRRC scheme.
5. STBC system is sensitive to the channel estimation errors and also it requires twice the pilot symbols as used in MRRC.

# *Chapter 4*

# WIRELESS FADING ENVIRONMENT

*This chapter gives a short introduction on the fading and the various types of multipath fading. The, main processes which are utilized to model the fading channel have also been discussed. The chapter includes the fundamental concepts of time-selective flat fading environment.*

## 4.1 Introduction to Fading

The fluctuations, occurring in signal power, due to changes in magnitude and phases resulting from multipath delay causes fading. Fading occurs due to the interference between variants of transmitted signals that arrive at the receiver at the distinct time intervals.

Three fundamental phenomena namely reflection, diffraction and scattering are described further. The electromagnetic waves interference is the main cause of reflection, which occurs when the dimension of the object is huge in comparison to the wavelength of the signal.

Diffraction is caused when the radio path between the transmitter and the receiver is hindered due to the indefinite edges. Fading occurs because of the absorption of radio frequency energy in the ionosphere. Multipath fading is the result of reflections due to the ground and surrounding systems.

### 4.1.1 Fading Channels

- **Flat Fading Channel -** When the wireless channel bandwidth is more than the transmitted signal bandwidth, the channel is considered to be flat fading. Here, the gain remains constant for all the frequency components existing in a signal.
- **Frequency-Selective Channel –** When the wireless channel bandwidth is lower than the transmitted signal bandwidth, the channel is considered to be frequency-selective. Here, the gain does not remain constant for entire frequency components of the signal. The concept of ISI is introduced in this type of fading channel.
- **Fast Fading Channel -** When the channel's coherence time is less than the transmitted signal's symbol period, it results in fast-fading. The Doppler spread is caused due to the frequency dispersion.

- **Slow Fading Channel -** When channel's coherence time is greater than the transmitted signal's symbol period, it results in slow fading. Here, the Doppler spread of the channel is much less, when compared with the bandwidth of the baseband signal.

### 4.1.2 Fading Parameters

The different parameters of time-varying fading channels are given below

- **Multipath Time Delay Spread** - It is represented as the temporal difference amid the first signal component and the last signal component received.
- **Coherence Bandwidth** - It is described as the range of frequencies over which two signals are highly correlated, which means that the channel turns out to be equal for both of the signals.
- **Coherence Time** - It is expressed as the time interval over which the channel gain remains constant. Due to the time-varying behavior of the channel, coherence time comes into the picture.
- **Doppler Spread** - When the spectral expanding occurs because of time-varying nature of the channel and is described as the spectrum of frequencies, for which the Doppler spectra received is extensively non-zero.

### 4.1.3 Path Loss

The increase in the distance between the transmitter and receiver results in the decrease of average strength of the signal. Thus, path loss can be termed as the difference in the transmitted signal power and the received signal power. This represents the signal attenuation which is measured in dB, and is a positive quantity.The received signal strength turns out to be inversely proportional to the square of the frequency and the distance which is given as

$$P_{\mathrm{Rec}} \alpha \frac{GP_T}{f^2 D^2} \tag{4.1}$$

where, $P_{\mathrm{Rec}}$ represents the received power, $P_T$ represents the transmitted signal strength, $f$ represents the frequency of the carrier signal, $D$ represents the distance between transmitting and receiving antenna, $G$ gives the power gain of the transmitting antenna. The free space path loss model is shown as [8].

$$PL(dB) = 10\log\frac{P_T}{P_R} = -10\log\left[\frac{G_T G_R \lambda^2}{(4\pi)^2 D^2}\right] \tag{4.2}$$

where, $\lambda$ is wavelength of the transmitted signal and $PL$ represents the path loss in the channel in dB.

## 4.2 Multipath Fading Parameters

When multipath segments exist, fading is consistently prompt. Multiple segments arriving at the receiving antenna at somewhat distinct time intervals result in fading. Considering both the transmitter and receiver segments to be in motion, a phase difference exist between the received signals, which results in the frequency shifting. Power-delay-profile (PDP) of the channel defines all of these parameters. PDP results in plotting the received power as a function of mean excess delay against the fixed delay interval.

Parameters can be defined as

1. Time Dispersion Parameters
2. Frequency Dispersion Parameters

### 4.2.1 Time Dispersion Parameters

- Mean Excess Delay
- Root Mean Square Delay Spread
- Maximum Excess Delay
- Coherence Bandwidth

*4.2.1.1 Mean Excess Delay* ($\overline{\tau}$)

Here, the mean excess delay is resolved with the help of parameters of power delay. $\overline{\tau}$ can be defined as the first moment of PDP. $\overline{\tau}$ can be mathematically represented as

$$\overline{\tau} = \frac{\sum_m g_m^2 \tau_m}{\sum_m g_m^2} = \frac{\sum_m P(\tau_m)\tau_m}{\sum_m P(\tau_m)} \tag{4.3}$$

where, $g_m$ represents the path gain, $\tau_m$ represents the delayed path and $g_m^2$ represents the power associated with the $m^{th}$ multipath.

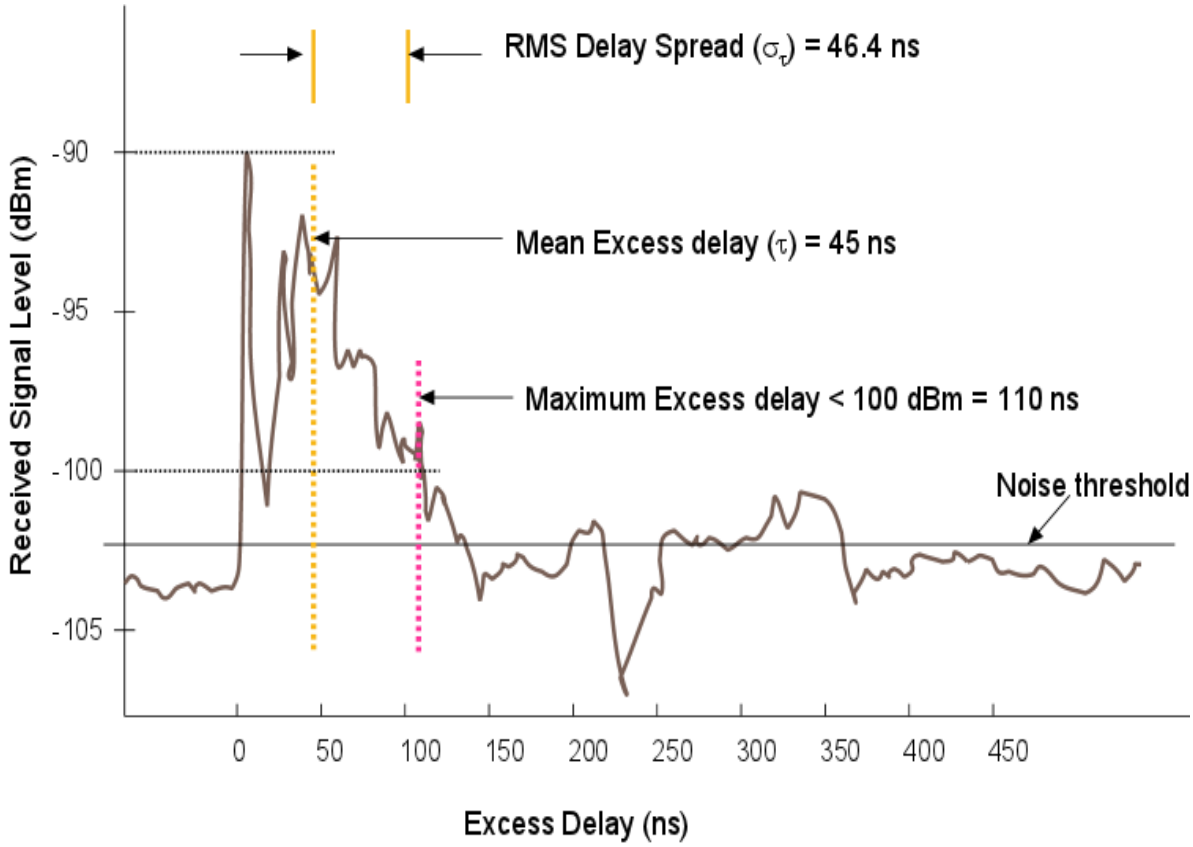


**Fig. 4.1.** Power delay profile parameters [8].

*4.2.1.2 Root Mean Square Delay Spread* ($\sigma_{rms}$)

Root mean square delay spread can be represented as the square root of second central moment function of PDP. $\sigma_{rms}$ can be mathematically represented as

$$\sigma_{rms} = \sqrt{\overline{\tau^2} - \left(\overline{\tau}\right)^2} \tag{4.4}$$

where, $\overline{\tau^2}$ is given by

$$\overline{\tau^2} = \frac{\sum_m g_m^2 \tau_m^2}{\sum_m g_m^2} = \frac{\sum_m P(\tau_m)\tau_m^2}{\sum_m P(\tau_m)}$$

where, $\sigma_{rms}$ represents the root mean square delay spread occurring in the wireless phenomenon and $\bar{\tau}$ represents the mean excess delay spread.

*4.2.1.3 Maximum Delay Spread* $(\tau_{\max})$

It is calculated when the first arriving component is received at $\tau_0$ and the last arriving component is received at $\tau_{L-1}$ and L can be demonstrated as the length of delay spread in PDP then maximum delay spread is calculated as

$$\tau_{\max} = \tau_{L-1} - \tau_0 \tag{4.5}$$

*4.2.1.4 Coherence Bandwidth* $(B_c)$

The measure of a group of frequencies calculated by enumeration data sets, for which the channel response is said to be flat, represents the coherence bandwidth. For this range, all the spectral components are passed as it is through the channel. Here, the channel responds equally to all the components and passes them with the equal gain as well as linear phase. It is determined that at the coherence bandwidth, the frequency components achieves amplitude correlation. $B_c$ denotes the coherence bandwidth. If $B_c$ is defined as the group of frequencies, which considers the frequency correlation function to be more than 0.9 then $B_c$ is given as

$$B_c = \frac{1}{50\sigma_{rms}} \tag{4.6}$$

Here, $\sigma_{rms}$ can be represented as root mean square delay spread.

Considering the correlation function to be more than 0.5

$$B_c = \frac{1}{5\sigma_{rms}} \tag{4.7}$$

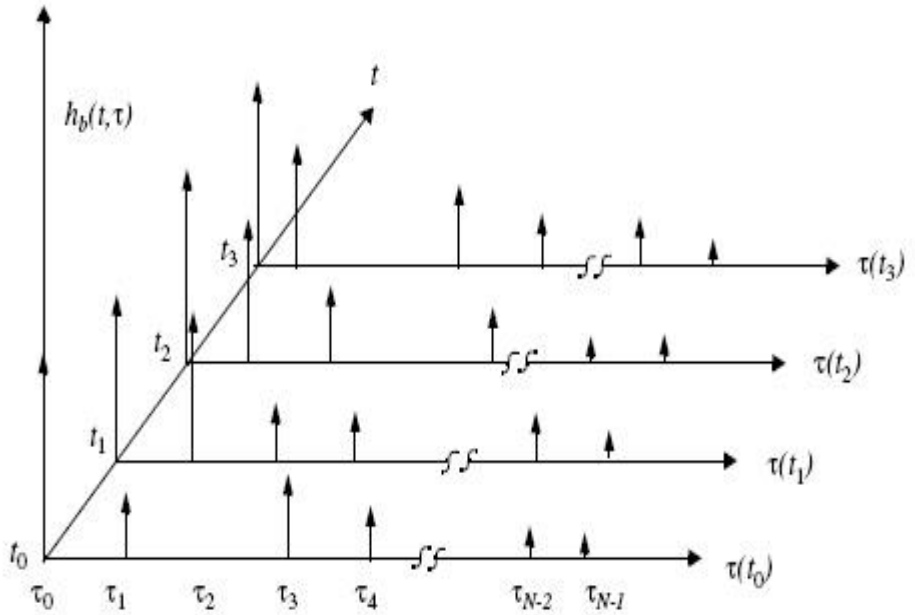


**Fig. 4.2.** Time-varying nature of the channel [8].

### 4.2.2 Frequency Dispersion Parameters

- Doppler Spread
- Coherence Time

#### *4.2.2.1 Doppler Spread* $(B_D)$

When the channel is time varying, i.e., when there exist motion amid transmitter and receiver and or when the motion of objects amid them, Doppler spread comes into the picture. $B_D$ is defined as the measure of spectral widening, which occurs when the mobile radio channel changes with respect to the time. When the bandwidth of the baseband signal $(B_s)$ is greater than the Doppler effects, it represents the slow fading. When the bandwidth of the baseband signal $(B_s)$ is less than the Doppler spread effects on the receiver, it represents the fast fading.

#### *4.2.2.2 Coherence Time* $(T_c)$

Coherence time can be defined as the enumerated time duration for which the channel impulse response remains static. For this time duration, the received signal components may

be highly correlated. When the inverse of the bandwidth of the message signal greater than the $T_c$, it results in the distortion on the receiver side.

$$T_c \approx \frac{1}{f_D} \tag{4.8}$$

where, $f_D$ represents Doppler shift.

## 4.3 Multipath Propagation

In the wireless communication, the multipath phenomenon occurs due to the presence of a non line-of-sight (LOS) communication or when there exist obstructions in the communication path. The reflecting matters and scatterers present in the communication channel result in a varying environment, which dissipate the energy of the signal in magnitude, phase and time. This results in the arrival of multiple delayed versions of the signal, which is distorted in any sense due to wireless propagation. Radio communication system is designed using multipath propagation model. Multipath signal will reach the receiver through many terrestrial radio communication system. Multipath reflection occurs due to hills, trees, buildings, towers, vehicles etc. Fig. 4.3 depicts the multipath propagation effects due to reflection.

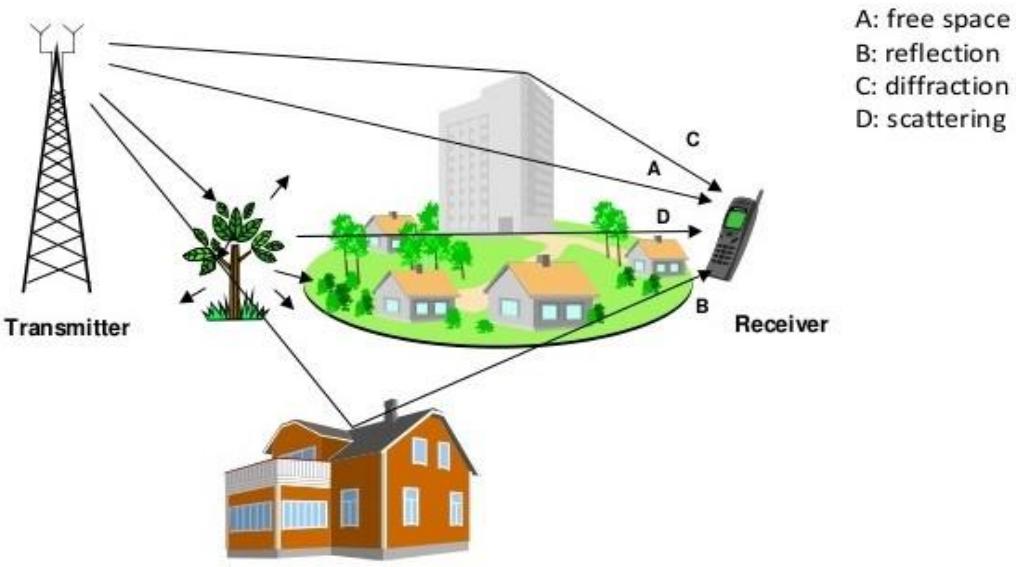


**Fig. 4.3.** Multipath propagation effect [8].

The summation of the signals is performed at the receiver. All the signals are received from the independent paths, traveling through the different paths the resulting signal may add constructively or subtract destructively depending on the phases of the received signal.

In most cases signal will be change with relative path lengths. Due to the movement of transmitter and receiver, or due to motion between obstacles, which provide reflecting surface, multiple paths originate. Thus, this will result in the change in relative path lengths and arrival time of the signal at the receiver and thus, signal will be summed together with the error associated with it leads to the signal fading. This results in several problems, includes phase distortion and ISI. Thus, it becomes important for inclusion of some techniques,to diminish the effects caused by fading. Further, we will consider the various types of multipath fading.

### 4.3.1 Types of Multipath Fading

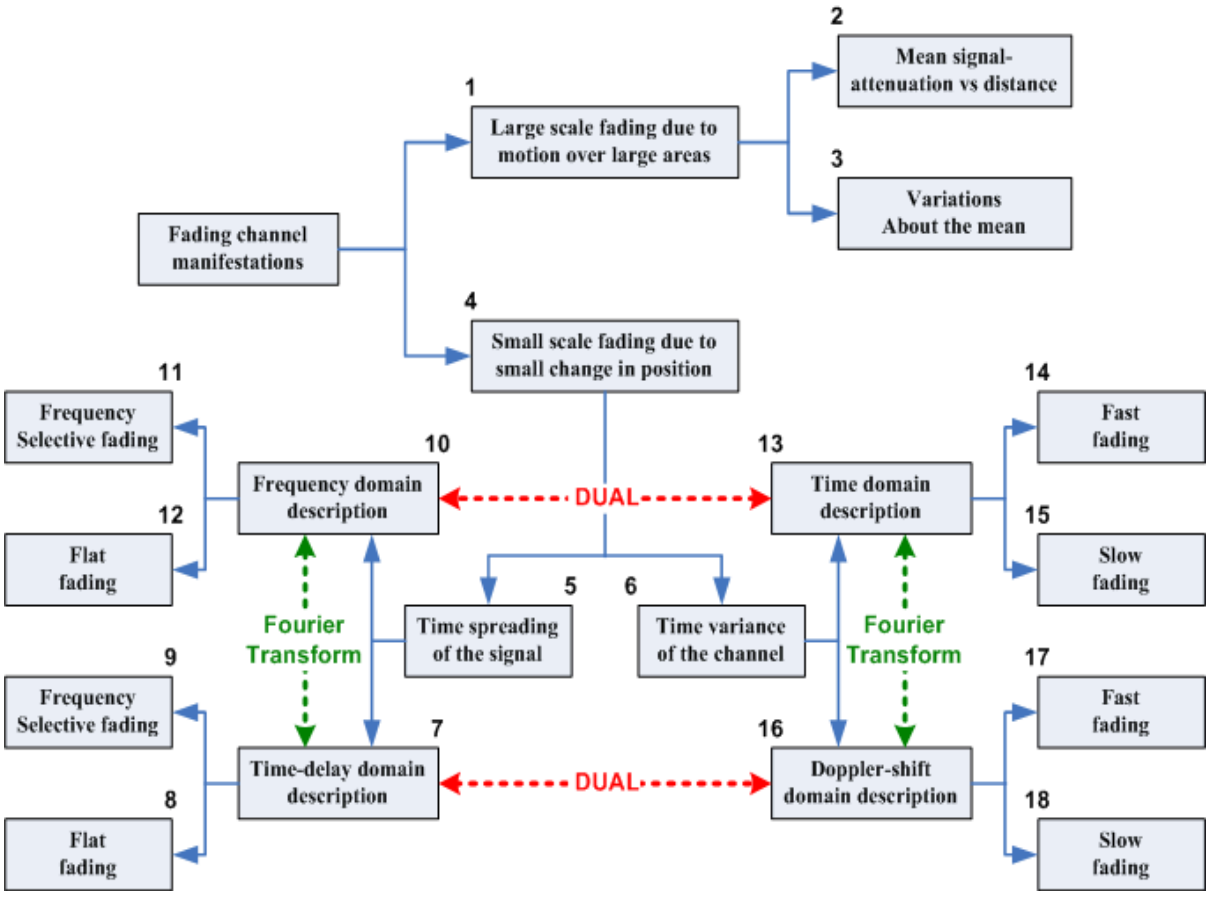


**Fig. 4.4.** Types of multipath fading [8].

Generally, the focus is on determining the strength of the average received signal present at a defined distance from the transmitter for the propagation models. It also focuses on the inconsistency of the signal strength at a particular location in a closed dimensional area. Fig. 4.4 represents the various types of multipath fading. It can be generally classified into two types

- Large-Scale Fading
- Small-Scale Fading

*4.3.1.1 Large-Scale Fading*

Propagation models play a vital role in the prediction of the average signal power from a random transmitter-receiver antenna. Considering the signal strength for a large-scale propagation model, which is represented by large distance amid transmitter and receiver separation, it may be of the order of several hundreds or thousands of meters. With the motion of the mobile object over a larger distance, the received signal strength will considerably reduce. It is mainly because of the penetration of radio frequency energy in the ionosphere. Reflection, diffraction, and scattering are the three types of absorption.

Hata Model, Knife-edge diffraction model, Okumura model, Longley-Rice model are some different types of fading models, which represent the effects of large-scale fading.

*4.3.1.2 Small-Scale Fading*

Considering very small separation amid transmitter and receiver, the small-scale fading has been discussed. Due to the movement of the mobile device, the instantaneous received signal strength oscillates, which results in small-scale fading. Even when the receiver moves only a fraction of wavelength distance, the received signal strength varies by three or four orders of magnitude (30 dB or 40 dB) for small-scale fading. Fig. 4.5 shows small and large scale fading changing with the distance between the transmitter and receiver. Further small-scale fading is divided into four types, which are explained further as flat fading, frequency- selective fading, fast fading, and slow fading.

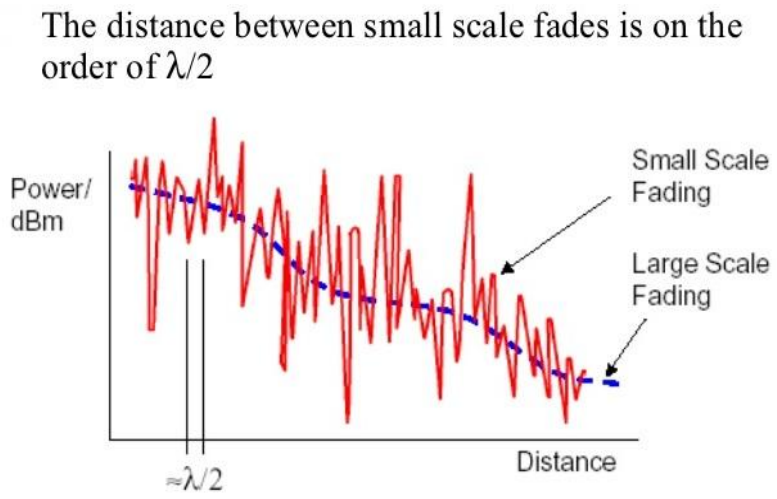


**Fig. 4.5.** Small-scale and large-scale fading [8].

## 4.4 Types of Small-Scale Fading

Transmitted signal characteristics are affected, when it propagates through the channel. Small signal fading is dependent upon the signal specifications like bandwidth as well as the symbol period. It is also dependent upon the channel parameters like root mean square delay spread as well as Doppler shift. Fig. 4.9 shows the different types of small-scale fading. Here, the main discussion is done for four different types of fading.

- Flat Fading
- Frequency Selective Fading
- Fast Fading
- Slow Fading

### 4.4.1 Flat Fading

When the channel experiences a steady gain and undeviating phase response over a band of frequencies, which is more than the bandwidth of the transmitted signal it results in flat fading experienced at the receiver. For flat fading, all the original features of the transmitted signal are retained at the receiver. Magnitude response of the received signal changes due to multipath which causes the deviation in the gain of the channel. The received signal experiences flat fading if and only if

$$B_S << B_C \tag{4.9}$$

and

$$T_S >> \sigma_{rms} \tag{4.10}$$

where, $T_S$ represents the inverse of the bandwidth of the baseband signal, $B_S$ represents the bandwidth of the transmitted signal, $\sigma_{rms}$ represents the root mean square delay spread and $B_C$ represents the coherence bandwidth.

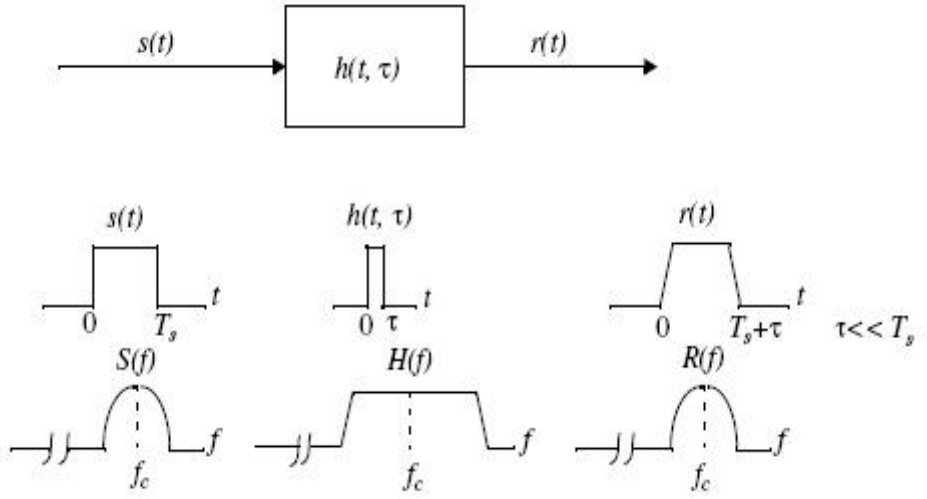


**Fig. 4.6.** Flat fading [8].

### 4.4.2 Frequency-Selective Fading

When the channel experienced by the received signal has a steady gain as well as linear phase response over a bandwidth, which is less than the bandwidth of the transmitted signal, This results in frequency-selective fading. Here, the characteristics of the original signal are not retained at the receiver. ISI occurs in this type of the fading. Fluctuations in the received signal gain due to multipath causes the change in the amplitude of the received signal. Received signal experiences frequency-selective fading if and only if

$$B_S > B_C \tag{4.11}$$

and

$$T_S < \sigma_{rms} \tag{4.12}$$

where, $T_S$ represents the inverse of the bandwidth of the baseband signal, $B_S$ represents the bandwidth of the transmitted signal. Here, $\sigma_{rms}$ represents the root mean square delay spread and $B_C$ represents the coherence bandwidth.

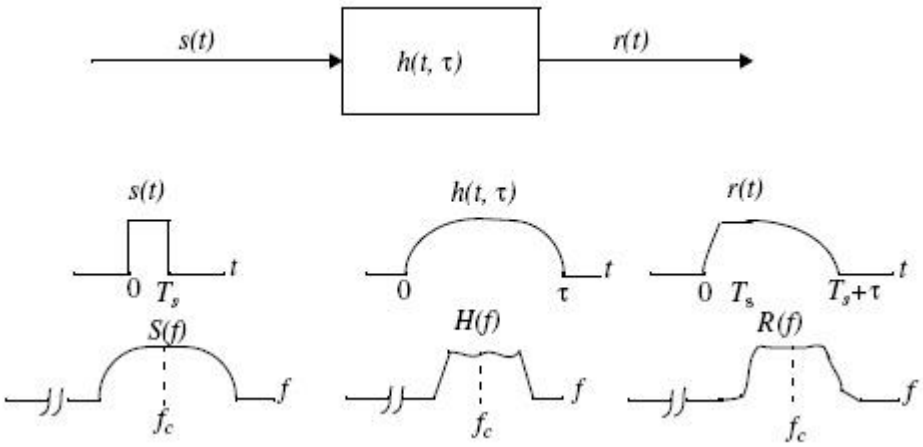


**Fig. 4.7.** Frequency-selective fading [8].

### 4.4.3 Fast Fading

In the fast fading, the rate of change of the transmitted signal and the rate of change of the channel is compared. Fast fading is dependent on this change. Here, channel impulse response is varied rapidly within the symbol period duration. Doppler spreading that leads to frequency dispersion results in high distortion of the signal. With the increase in the Doppler spread, an increase in the signal distortion occurs. Received signal experiences fast fading if and only if

$$T_S > T_C \tag{4.13}$$

and

$$B_S < B_D \tag{4.14}$$

where, $T_S$ represents the inverse of the bandwidth of the baseband signal and $T_C$ represents the coherence time. Here, $B_D$ represents the Doppler spread and $B_S$ is the transmitted signal bandwidth.

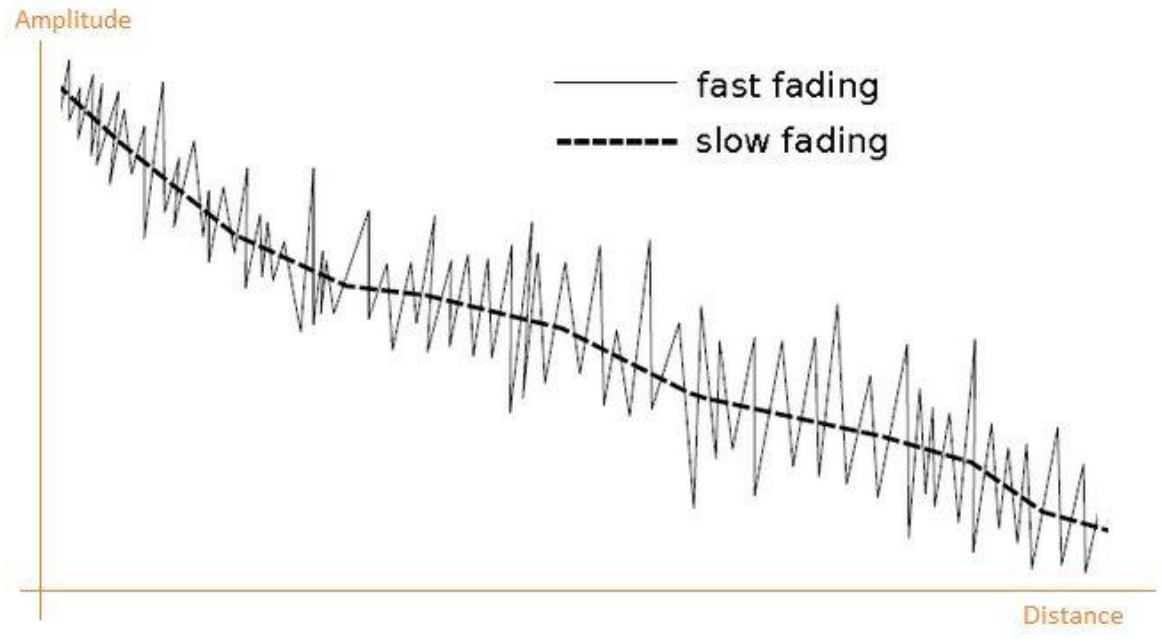


**Fig. 4.8.** Fast and slow fading [8].

### 4.4.4 Slow Fading

For the slow fading, change in the channel impulse response is much sluggish than the transmitted message signal. Here, the Doppler spread of the channel is much lower when compared to the bandwidth of the message signal. Received signal experiences slow fading if and only if

$$T_S << T_C \tag{4.15}$$

and

$$B_S >> B_D \tag{4.16}$$

where, $T_S$ represents the inverse of the bandwidth of the message signal and $T_C$ represents the coherence time. $B_D$ represents the Doppler spread, whereas $B_S$ represents the transmitted signal bandwidth.

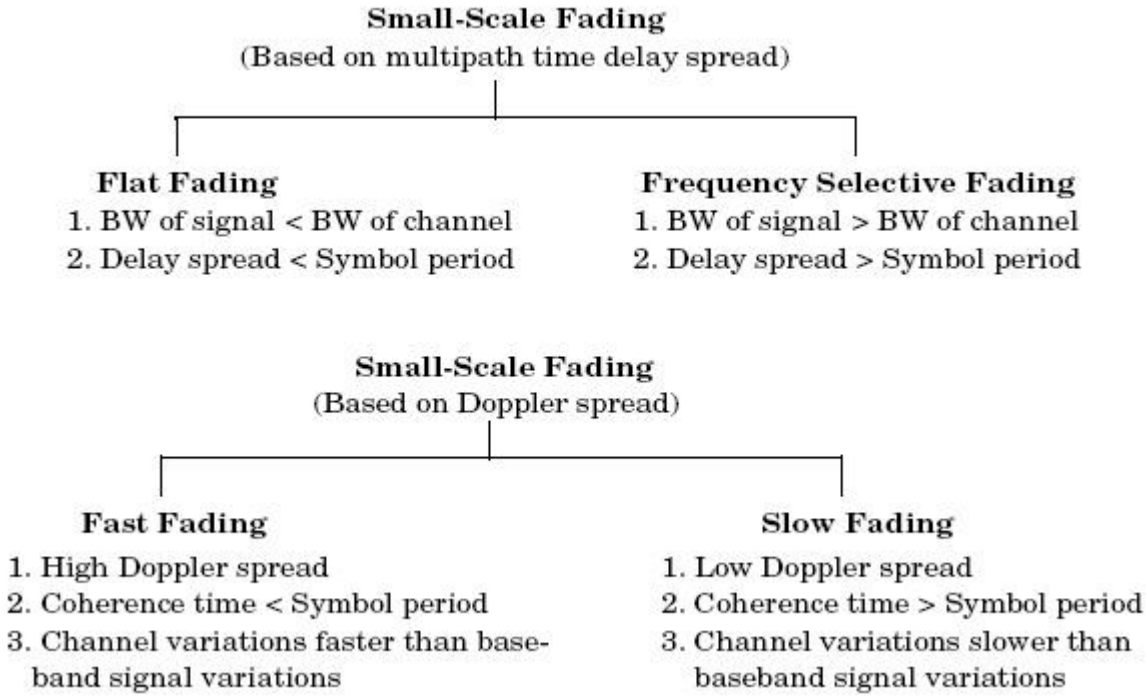


**Fig. 4.9.** Types of small-scale fading [8].

In the multipath channel, the small scale fading occurrence statistically obeys the different features of different random processes such as Rayleigh, Rician, Nakagami etc.

## 4.5 Different Types of Random Processes

There exist many important types of random processes in the wireless applications, those are useful to design different systems. A reliable communication link can be designed using these random processes between the transmitter and receiver side. It is dependent on the time-varying analytical behavior of the existing channel. Generally, random processes used are

- Rayleigh random process
- Rician random process

### 4.5.1 Rayleigh Random Process

Rayleigh distribution can be expressed as the envelope obtained by the summation of two quadrature Gaussian noise signals. It describes the analytical time-varying nature of the received envelope of the flat-fading channel and/or the envelope of an indiviual multipath segment [8]. Fig. 4.10 describes the PDF and cumulative-distribution-function (CDF) of a

Rayleigh distributed random variable $X$. The Rayleigh distribution PDF and CDF are mathematically shown as

$$f_X(x) = \left(\frac{x}{\sigma^2}\right)\exp\left(-\frac{x^2}{2\sigma^2}\right)u(x) \tag{4.17}$$

$$F_X(x) = \left(1-\exp\left(-\frac{x^2}{2\sigma^2}\right)\right)u(x) \tag{4.18}$$

The time-varying nature of the channel is normally determined using Rayleigh distribution. Fading affects the received signal strength which can be depicted with the probability of the signal level. Table 4.1 gives the signal level probability of the Rayleigh distribution.

| **Signal level (dB)** | **% Probability of Signal Level** |
|---|---|
| 10 | 99 |
| 0 | 50 |
| -10 | 5 |
| -20 | 0.5 |
| -30 | 0.05 |

**Table 4.1.** Probability of signal level in the Rayleigh distribution [8].

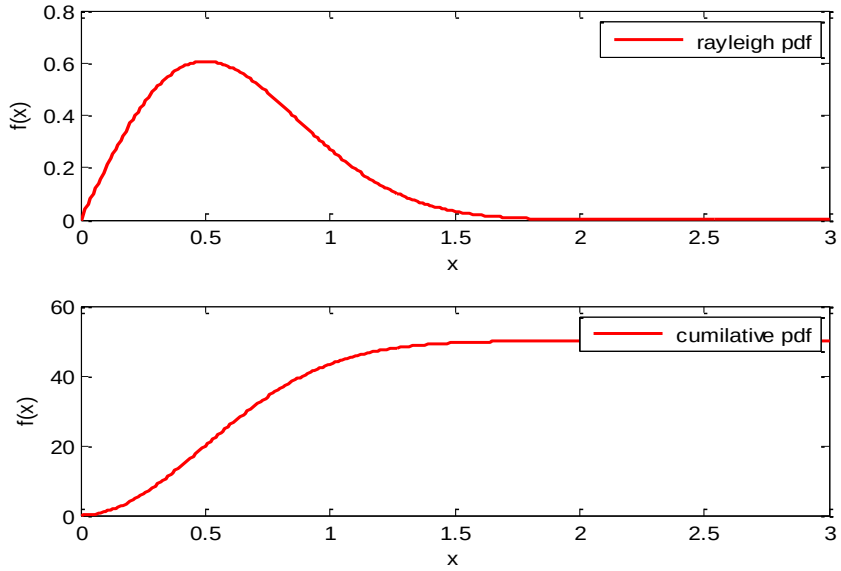


**Fig. 4.10.** PDF and CDF of a Rayleigh random variable with $\sigma$ = 0.707 [8].

### 4.5.2 Rician Random Process

Rician fading model is almost similar to Rayleigh fading model. The only thing that varies is the strong prevalent element present in Rician fading. This dominant component happens to be the LOS wave. Rician models consider that

- the prevalent wave may be the phasor summation for two or more dominant signals, e.g. the line-of-sight, or a ground reflection. Thus, the mixed signal is then generally taken as a determinable process.
- the prevalent wave may also be subjected to shadowing effect. This becomes a preferred assumption for the modeling of the satellite channels.

In addition to the dominant element, the mobile antenna may be receiving large number of reflected and scattered waves.

- **PDF of Signal Amplitude**

The amplitude of the signal is more involved in the derivation of the PDF for Rician fading than Rayleigh fading. Here, a Bessel function appears in the mathematical definition. This expression can be efficiently estimated by Nakagami fading model, but the practice of Rician and Nakagami fading is necessarily distinct for the deep fades.

The Rician distribution PDF is mathematically shown as

$$f_X(x) = \left(\frac{x}{\sigma^2}\right)\exp\left(-\frac{x^2+a^2}{2\sigma^2}\right)\mathrm{J}_o\left(\frac{xa}{\sigma^2}\right) \tag{4.19}$$

where, $a$ represents the mean and $\sigma$ represents the RMS delay spread.

- ***K* Factor**

The Rician *K*-factor can be represented as the ratio of signal strength in prevalent component to the local-average scattered power. For the indoor medium, considering an unobstructed LOS amid the transmit and receive antenna, the *K*-factor is said to be in between 4dB and 12dB. When *K*-factor is equal to zero, Rayleigh fading is recovered.

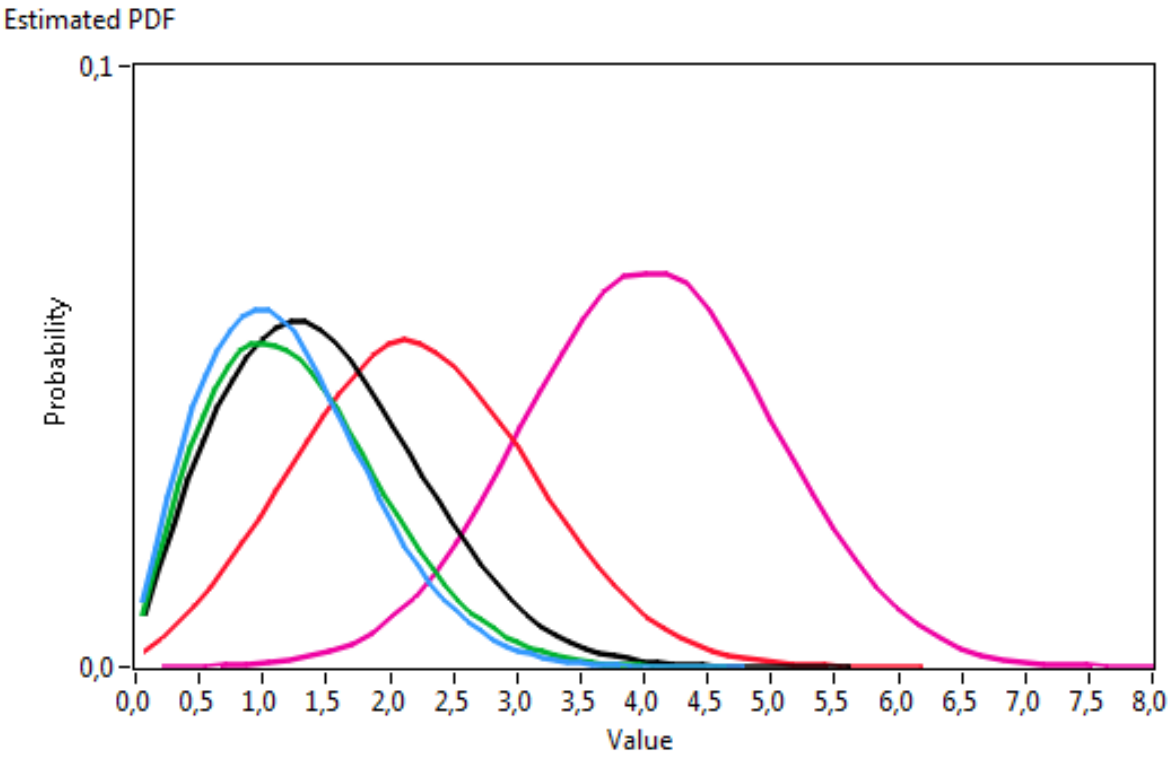


**Fig. 4.11**. Rician distribution with different values of K [8].

*Chapter 5*

# HIGH-RATE STBC COMMUNICATION SYSTEM USING IMPERFECT CSI WORKING UNDER TIME-SELECTIVE FLAT-FADING CHANNEL

*This chapter discusses the high-rate STBC system under Rayleigh multipath fading channel. Here, we have evaluated the performance of throughput curves and SER performance under perfect and imperfect CSI. In this, comparison two wireless systems namely high-rate (5/4) and (9/8) STBC schemes have been discussed along with rate-one STBC (Liu and Alamouti) in this thesis report to understand their performance in different conditions with different parameters.*

## 5.1 Introduction

In the wireless communication scenario, STBC is highly utilized for high data rate applications [2]. Its visualization can be done as an ideal technology and is used in the wireless local area in addition to third generation networks and in many latest applications. STBC system benefits include its robustness to multipath distortions and increased capacity. Generally, channel noise affects the STBC communication systems, mainly in the urban environment. The benefit of MIMO-STBC over single transmission link is its effectiveness to reduce the effects of multipath distortion. STBC system functions are usually affected by the fading phenomenon. Achieving reliable communication in STBC is more demanding because the received signals from multipath may produce destructive results. In STBC system, the type, origin and prophecy of the fading environment and noise sources are crucial to evolve the efficient methods to mitigate BER or SER.

The STBC system is the multichannel system and due to this, it is more resistant to the fading when compared to the single channel system. If one of the transmit chains is under deep fade then other transmit chain may still transmit the data efficiently [1]. One of the problems in the STBC system arises due to the CSI. The performance of STBC system and mostly space-time codes relies on careful channel estimation. It needs the introduction of the pilot symbols when the channel is highly time-varying. The proposed study is to evaluate the

performance of high data rate $(5/4)$ STBC system in a time-selective environment with CSI imperfections. First, the calculation of the performance of high rate system is done under perfect CSI in the time-selective environment working in Rayleigh multipath fading channel.

For multiple antennas data rate can be increased on the basis of spatial multiplexing and transmission is based on the quaternions for $2\times 2$ orthogonal code ($Q$ and $\overline{Q}$) which is shown as in Eq. (3.22)

where, $Q$ is the complex orthogonal design discovered by Alamouti, where $(.)^*$ represents the complex conjugate transpose. $\overline{Q}$ is a set of $x$ which is given by $2\times 2$ orthogonal matrices as shown in Eq. (3.23)

where, $\overline{Q}$ is the coset of $Q$.

However, the performance can degrade exponentially, when the channels are highly time-varying. The SER performance is mainly dependent on the value of Rayleigh fading parameter, which analyzes that when fading parameter is decreased SER performance degrades. STBC receiver works with the CSI imperfections to evaluate the transmitted signal from the received data.

## 5.2 Model of High-Rate $(5/4)$ STBC System with Rayleigh Channel in Time-Selective Environment

Here, the model of STBC system for transmission as well as reception is discussed. Fig. 5.1 depicts a wireless communication system with two-transmitter antennas and one-receiver antenna. Here, the information symbols are transmitted using Liu rate-one [7] technique with selective power scaling, so as to achieve high transmission rate. The channel is assumed to be Rayleigh flat-fading. The resulting two streams are transmitted from two antennas simultaneously. In the STBC system, first, the information data bits are to be made baseband modulated symbols $\{s_k\}$ by mapping and using QPSK or in general M-ary PSK. Usually, QPSK modulation is used in the STBC communication system, so each element in the STBC symbol is a complex number representing the particular QPSK constellation point.

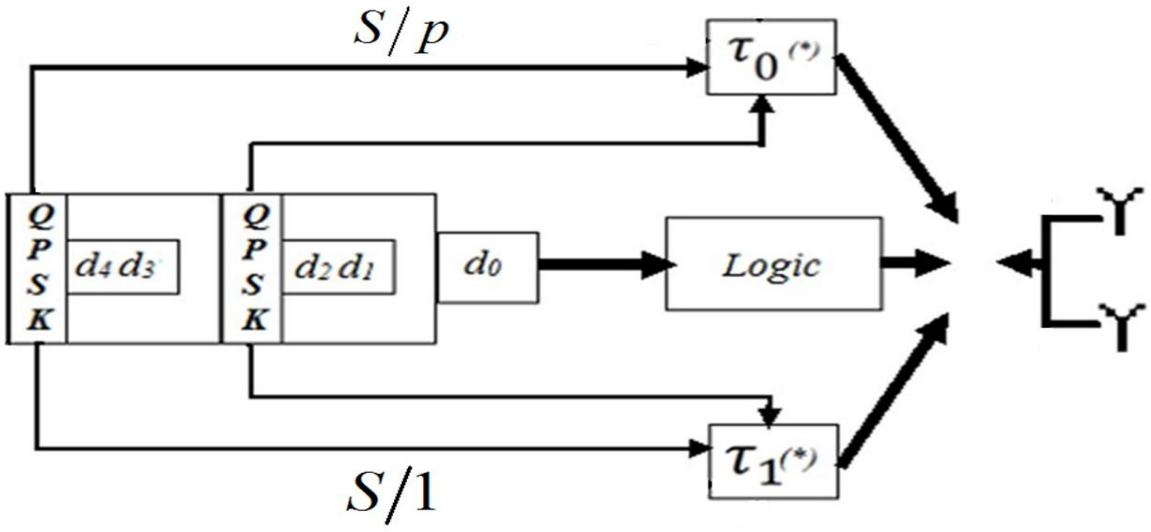


**Fig 5.1.** Block diagram of the data-rate (5/4) STBC system using QPSK modulation [4].

At the receiving antenna, matched filtering is done so as to recover the original data from the space-time encoded transmitted data. Here, we are considering the high-rate (r >1) for $2\times1$ and $4\times1$ antennas to estimate the channel parameters in a time-selective manner.

A frame of 5 bits is considered, and out of which four bits are paired as $\{d_1, d_2\}, \{d_3, d_4\}$. These pairs are mapped on QPSK constellation to generate the information symbols $s_i$. The bit $d_o$ is used to decide about the selective power scaling. Here, the effective throughput [1], [4] is defined as

$$\text{Effective Throughput} = (1-FER)\times \mathrm{R}_{STBC}\times Log_2(M) \tag{5.1}$$

where, $FER$ denotes the frame error rate, $R_{STBC}$ and $M$ denotes the code rate and constellation size respectively.

In this communication system with $d_o = 0$ and power scaling by $1/p$ through $\tau_0(.)$, the two consecutive signal/symbol samples are represented as

$$S_T = \frac{S}{p} \tag{5.2}$$

where, $p > 1$

In this communication system with $d_o = 1$ and power scaling by unity through $\tau_1(.)$, the two consecutive signal/symbol samples are represented as

$$S_T = \frac{S}{1} \tag{5.3}$$

In time selective but frequency-flat manner, two consecutive samples sent from the transmitter antenna to the receiver antenna as shown in [1] and [7],

$$r(2k) = h_1(2k)s(2k) + h_2(2k)s(2k+1) + \eta(2k) \tag{5.4}$$

$$r(2k+1) = -h_1(2k+1)s^*(2k+1) + h_2(2k+1)s^*(2k) + \eta(2k+1) \tag{5.5}$$

where, $r(.)$ represent the consecutive received samples, $h_i(.)$ denotes the channel coefficients from the $i^{th}$ transmit antenna to the receiving antenna. Channel coefficients are assumed to be flat-fading slowly time-varying, which follow first-order AR process, $s(.)$ represent the QPSK modulated symbols, $\eta(.)$ denotes the AWGN with zero mean and $\sigma^2$ variance. Mathematically, in [7], $h_i(.)$ is shown as

$$h_i(k) = \overline{h_i}(k)\exp(j2\pi f_o T_S k) \tag{5.6}$$

Here, $\overline{h_i}(k)$ arises due to Doppler shift and exponential factor arises due to frequency mismatch between oscillators of transmitter and receiver. According to Jakes' model [9]

$$E\left[\overline{h_i}(k)\overline{h_i}^*(k-1)\right] = J_o(2\pi f_d T_s) \tag{5.7}$$

Substituting Eq. (5.6) into Eq. (5.7) we get

$$E\left[h_i(k)e^{-j2\pi f_o T_s k}h_i^*(k-1)e^{j2\pi f_o T_s (k-1)}\right] = J_o(2\pi f_d T_s)$$

$$E\left[h_i(k)e^{-j2\pi f_o T_s k}h_i^*(k-1)e^{j2\pi f_o T_s k}e^{-j2\pi f_o T_s}\right] = J_o(2\pi f_d T_s) \tag{5.8}$$

To model channel coefficient as first-order AR process, we define channel as [7]

$$h_i(k) = \alpha h_i(k-1) + v_i(k) \tag{5.9}$$

Since $\alpha = E\left[h_i(k)h_i^*(k-1)\right]$ (5.10)

where, $E(.)$ denotes expectation operator [10].

Our aim is to find $\alpha$, i.e., fading parameter. Substitute Eq. (5.10) into Eq. (5.8) to get

$$\alpha \exp(-j2\pi f_o T_s) = J_o(2\pi f_d T_s)$$

We get, $\alpha = J_o(2\pi f_d T_s)\exp(j2\pi f_o T_S)$ (5.11)

Now, the data is transmitted with the help of extra information bit as shown in Fig. 5.1

If $d_o = 0$,

$$\vec{R}_{2k,2k+1} = \vec{H}_{2k,2k+1}\vec{S}_{2k,2k+1} + \vec{\eta}_{2k,2k+1} \tag{5.12}$$

which is the vector representation of Eq. (5.4) and Eq. (5.5)

where,

$$\vec{R}_{2k,2k+1} = \begin{bmatrix} r(2k) \\ r^*(2k+1) \end{bmatrix} \tag{5.13}$$

$$\vec{H}_{2k,2k+1} = \begin{bmatrix} h_1(2k) & h_2(2k) \\ h_2^*(2k+1) & -h_1^*(2k+1) \end{bmatrix} \tag{5.14}$$

$$\vec{\eta}_{2k,2k+1} = \begin{bmatrix} \eta(2k) \\ \eta^*(2k+1) \end{bmatrix} \tag{5.15}$$

and

$$\vec{S}_{2k,2k+1} = \begin{bmatrix} \frac{s(2k)}{p} \\ \frac{s(2k+1)}{p} \end{bmatrix} \tag{5.16}$$

where, $p$ is the real scalar, whose value is greater than '1'. $\vec{S}_{2k,2k+1}$ is the transmitted symbol signal matrix with zero-mean and variance $\sigma_s^2/p^2$ with the real scalar $p$ >1. Here, the symbols $s(2k)$ and $s(2k+1)$ are scaled by the factor $1/p$ to attain the selective power scaling, so as to achieve the full diversity, which is identical to the radius of the inner QPSK constellation circle, where $s(2k)$ and $s(2k+1)$ on the outer constellation circle have been normalized to unity, but due to power scaling factor average transmitted power has been reduced as compared to no scaling transmission. The PMPR attained for the transmitted signal is $p^2>1$ .

Now, received data is decoded by simple STBC decoding akin to Liu rate-one [7],

$$\vec{Z}_{2k,2k+1} = \hat{H}^{H}_{2k,2k+1}\vec{R}_{2k,2k+1} \tag{5.17}$$

But, $\hat{H}_{2k,2k+1} = H_{2k,2k+1} + \Delta\hat{H}_{2k,2k+1}$ , which arises because of imperfect channel estimation, where, $\Delta\hat{H}_k$ is the error in the estimation and is often expressed as AWGN with mean zero and variance $\sigma^2_{\Delta H_k}$. $\vec{Z}_{2k,2k+1}$ represents decoded data and $\hat{H}^{H}_{2k,2k+1}$ represents Hermitian of the estimated channel matrix, and is shown as

$$\hat{H}^{H}_{2k,2k+1} = \begin{bmatrix} \hat{h}_1^*(2k) & \hat{h}_2(2k+1) \\ \hat{h}_2^*(2k) & -\hat{h}_1(2k+1) \end{bmatrix} \tag{5.18}$$

Thus, on substituting values of Eq. (5.12) and Eq. (5.18) in Eq. (5.17), we get

$$\vec{Z}_{2k,2k+1} = \vec{\varphi}_{2k,2k+1}\vec{S}_{2k,2k+1} + \Delta\vec{\varphi}_{2k,2k+1}\vec{S}_{2k,2k+1} + \overrightarrow{WN}_{2k,2k+1} \tag{5.19}$$

where,

$$\vec{\varphi}_{2k,2k+1} = \begin{bmatrix} |h_1(2k)|^2 + |h_2(2k+1)|^2 & h_1^*(2k)h_2(2k) - h_1^*(2k+1)h_2(2k+1) \\ h_2^*(2k)h_1(2k) - h_1(2k+1)h_2^*(2k+1) & |h_2(2k)|^2 + |h_1(2k+1)|^2 \end{bmatrix}$$

$$\Delta\vec{\varphi}_{2k,2k+1} = \begin{bmatrix} \Delta h_1^*(2k)h_1(2k) + \Delta h_2(2k+1)h_2^*(2k+1) & \Delta h_1^*(2k)h_2(2k) - \Delta h_2(2k+1)h_1^*(2k+1) \\ \Delta h_2^*(2k)h_1(2k) - \Delta h_1(2k+1)h_2^*(2k+1) & \Delta h_2^*(2k)h_2(2k) + \Delta h_1(2k+1)h_1^*(2k+1) \end{bmatrix}$$

$$\overrightarrow{WN}_{2k,2k+1} = \begin{bmatrix} \eta(2k)\hat{h}_1^*(2k) + \eta^*(2k+1)\hat{h}_2(2k+1) \\ \eta(2k)\hat{h}_2^*(2k) - \eta^*(2k+1)\hat{h}_1(2k+1) \end{bmatrix}$$

Replacing $\Delta\overrightarrow{HN}_{2k,2k+1} = \Delta\vec{\varphi}_{2k,2k+1}\vec{S}_{2k,2k+1}$ (5.20)

Substituting value of Eq. (5.20) into Eq. (5.18), we get

$$\vec{Z}_{2k,2k+1} = \vec{\varphi}_{2k,2k+1}\vec{S}_{2k,2k+1} + \Delta\overrightarrow{HN}_{2k,2k+1} + \overrightarrow{WN}_{2k,2k+1} \quad (5.21)$$

Now in the case of $d_o = 1$, we consider $p = 1$ and the results are evaluated.

Also we get $Avg\left\{SNR_{d_o=0}\right\} = \dfrac{Avg\left\{SNR_{d_o=1}\right\}}{p^2}$ (5.22)

## 5.3 Model of High-Rate $(5/4)$ STBC System Working Under Imperfect CSI in Time-Selective Environment

In the last section, we have discussed the STBC for time-selective environment. But here, we will discuss high rate STBC system in which orthogonal designs for two transmit antennas are based on quaternion for two transmit antennas shown as [2]

$$\vec{Q}_1(s_1 s_2, d_o = 1) \rightarrow \begin{bmatrix} s_1 & s_2 \\ -s_2^* & s_1^* \end{bmatrix} \quad (5.23)$$

When the coset of $\vec{Q}_1$ is power scaled by $p$, we get

$$\frac{\vec{Q}_o(s_1 s_2, d_o = 0)}{p} = \begin{bmatrix} 1 & 0 \\ 0 & -1 \end{bmatrix}\vec{Q}_1(s_1 s_2, d_o = 1) = \begin{bmatrix} \frac{s_1}{p} & \frac{s_2}{p} \\ \frac{s_2^*}{p} & \frac{-s_1^*}{p} \end{bmatrix} \quad (5.24)$$

Thus on the basis of $d_o$ we are getting received signal as on the basis of above quaternions.

If $d_o = 1$ then,

The received signal can be mathematically shown as

$$r(2k) = h_1(2k)s(2k) - h_2(2k)s^*(2k+1) + \eta(2k) \tag{5.25}$$

$$r(2k+1) = h_2(2k+1)s^*(2k) + h_1(2k+1)s(2k+1) + \eta(2k+1) \tag{5.26}$$

Representing Eq. (5.25) and Eq. (5.26) in matrix form, we get

$$\begin{bmatrix} r(2k) \\ -r^*(2k+1) \end{bmatrix} = \begin{bmatrix} h_1(2k) & h_2(2k) \\ -h_2^*(2k+1) & h_1^*(2k+1) \end{bmatrix} \begin{bmatrix} s(2k) \\ -s^*(2k+1) \end{bmatrix} + \begin{bmatrix} \eta(2k) \\ -\eta^*(2k+1) \end{bmatrix} \tag{5.27}$$

Representing Eq. (5.27) in vector form, we get

$$\overrightarrow{RQ1}_{2k,2k+1} = \vec{H}_{2k,2k+1}\overrightarrow{SQ1}_{2k,2k+1} + \overrightarrow{WQ1}_{2k,2k+1} \tag{5.28}$$

If $d_o = 0$, then

$$r(2k) = h_1(2k)\frac{s(2k)}{p} + h_2(2k)\frac{s^*(2k+1)}{p} + \eta(2k) \tag{5.29}$$

$$r(2k+1) = h_2(2k+1)\frac{\left(-s^*(2k)\right)}{p} + h_1(2k+1)\frac{s(2k+1)}{p} + \eta(2k+1) \tag{5.30}$$

Representing above Eq. (5.29) and Eq. (5.30) in matrix form, we get

$$\begin{bmatrix} r(2k) \\ r^*(2k+1) \end{bmatrix} = \begin{bmatrix} h_1(2k) & h_2(2k) \\ -h_2^*(2k+1) & h_1^*(2k+1) \end{bmatrix} \begin{bmatrix} \frac{s(2k)}{p} \\ \frac{s^*(2k+1)}{p} \end{bmatrix} + \begin{bmatrix} \eta(2k) \\ \eta^*(2k+1) \end{bmatrix} \tag{5.31}$$

Representing above Eq. (5.31) in vector form, we get

$$\overrightarrow{RQ0}_{2k,2k+1} = \vec{H}_{2k,2k+1}\overrightarrow{SQ0}_{2k,2k+1} + \overrightarrow{WQ0}_{2k,2k+1} \tag{5.32}$$

Thus received vector can be represented as

$$\vec{R}_{2k,2k+1} \Rightarrow \left\{\overrightarrow{RQ0}_{2k,2k+1}, \overrightarrow{RQ1}_{2k,2k+1}\right\} \tag{5.33}$$

whereas decoding of the data is done as

$$\vec{Z}_{2k,2k+1} = \hat{H}^{H}_{2k,2k+1}\vec{R}_{2k,2k+1} \Rightarrow \left\{\hat{H}^{H}_{2k,2k+1}\overrightarrow{RQ0}_{2k,2k+1}, \hat{\mathrm{H}}^{H}_{2k,2k+1}\overrightarrow{RQ1}_{2k,2k+1}\right\} \tag{5.34}$$

where, $\hat{H}_{2k,2k+1} = \overrightarrow{H}_{2k,2k+1} + \Delta\overrightarrow{H}_{2k,2k+1}$

Here, we are getting one important result i.e., on putting $p = 1$, the same result is produced as in the case of $d_o = 1$, shown in Eq. (5.27) .Using simple mathematical computation, it can be analyzed that optimum value of $p$ is $\sqrt{3}$ [4].

Here, $\hat{S}_{2k,2k+1} \Rightarrow \left\{\hat{S}Q0_{2k,2k+1}, \hat{\mathrm{S}}Q1_{2k,2k+1}\right\}$, which denotes two candidate solutions obtained due to matched filtering.

Then, ML decoding is performed as

$$\min \left\| r(2k), r(2k+1) - \left[\hat{h}(2k), \hat{h}(2k+1)\right]\hat{S}_{2k,2k+1} \right\|^2 \tag{5.35}$$

This result of ML decoding thus performs the decoding of $d_o$ because through ML decoding, we can make the decision between $\vec{S}Q0_{2k,2k+1}$ or $\vec{S}Q1_{2k,2k+1}$.

## 5.4 Simulation Results and Discussion

The performance of the proposed scheme will be analyzed, while working under Rayleigh flat-fading channel in the time-selective environment using QPSK modulation. For simulations, we have considered a single antenna at the receiver. It is assumed that the total power is equally divided by the number of transmitting antennas. The receiver either has perfect or imperfect knowledge of the CSI under different conditions. In selective power scaling scheme, the value of $p$ is set at $\sqrt{3}$ [4].

Through simulations, it is shown that the proposed system's performance is favored by high SNR and low channel estimation errors. We will also compare the performance of underlying STBC scheme at different fading values of Rayleigh fading parameter alpha (i.e., α = 0.5, 0.75, 1) under perfect and imperfect CSI at the receiver. The performance of the high-rate STBC scheme is evaluated with computer simulations. These results are obtained for 4-PSK modulation system.

### 5.4.1 Performance Evaluation of Liu Rate-One and High-Rate $(5/4)$ $2\times1$ STBC System with Perfect CSI Under Time-Selective Environment

The simulation results for the $2\times1$ system with Rayleigh flat-fading channel analyzing the effects of channel estimations are presented in Fig. 5.2 and Fig. 5.3. It is illustrated from the figures that as the value of $|\alpha|$ decreases, systems effective throughput decreases and the value of SER increases. The performance of high-rate (5/4) STBC system is better when the number of iterations is increased and also the value of Rayleigh fading parameter is increased (up to 1) when evaluated under the perfect CSI. Here, Liu rate-one is defined in [7].

| Parameter | Value |
|---|---|
| Modulation used | QPSK |
| Number of transmitter and receiver antennas | $2\times1$ |
| Rayleigh fading parameter, $\|\alpha\|$ | 1, 0.75, 0.5 |

**Table 5.1.** System parameters for effective throughput of $2\times1$ STBC system under perfect CSI.

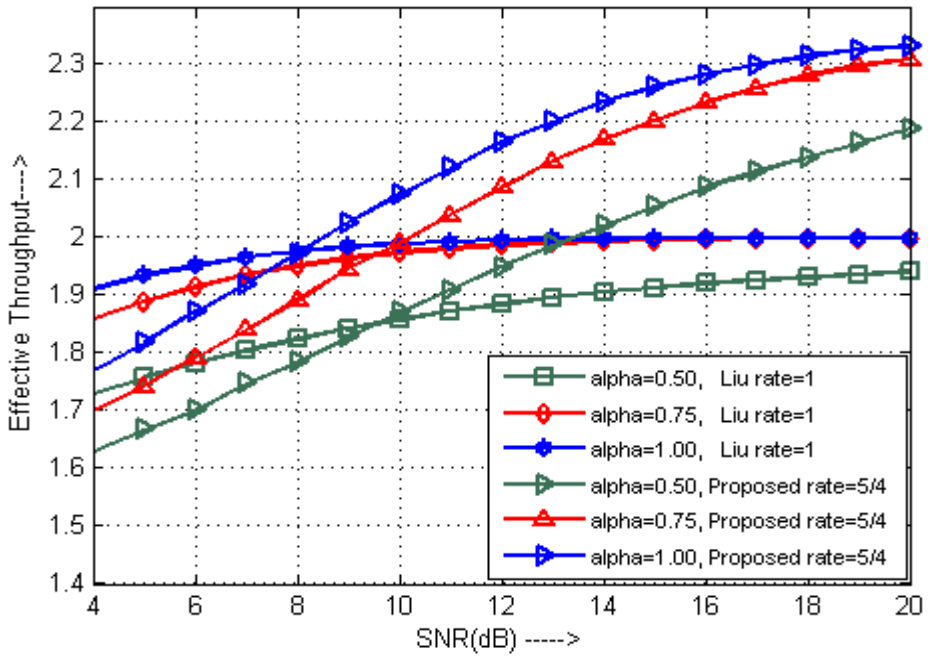


**Fig 5.2.** Effective throughput vs. SNR for different values of $|\alpha|$.

It is clear from the Fig. 5.2 that the crossover point for the proposed scheme $(5/4)$ $2\times1$ STBC system with $|\alpha|$=0.5 under time-selective environment is approximately 9.5dB SNR. Simulation results demonstrate that this system is favored by high SNR and low channel estimation error. High-rate $5/4$ STBC system achieves a throughput of 2.33; whereas for Liu rate-one STBC system [7], the maximum throughput is 2. Thus, the proposed STBC system outperforms the Liu rate-one STBC system [7] at the high SNR values, but at the cost of decoding complexity. The throughput of the high-rate $5/4$ STBC system supersedes the Liu rate-one STBC system [7] with $|\alpha|$ = 1 at approximately SNR = 8dB. For the SNR values higher than this crossover point the throughput of the proposed system increases with the increasing values of SNR.

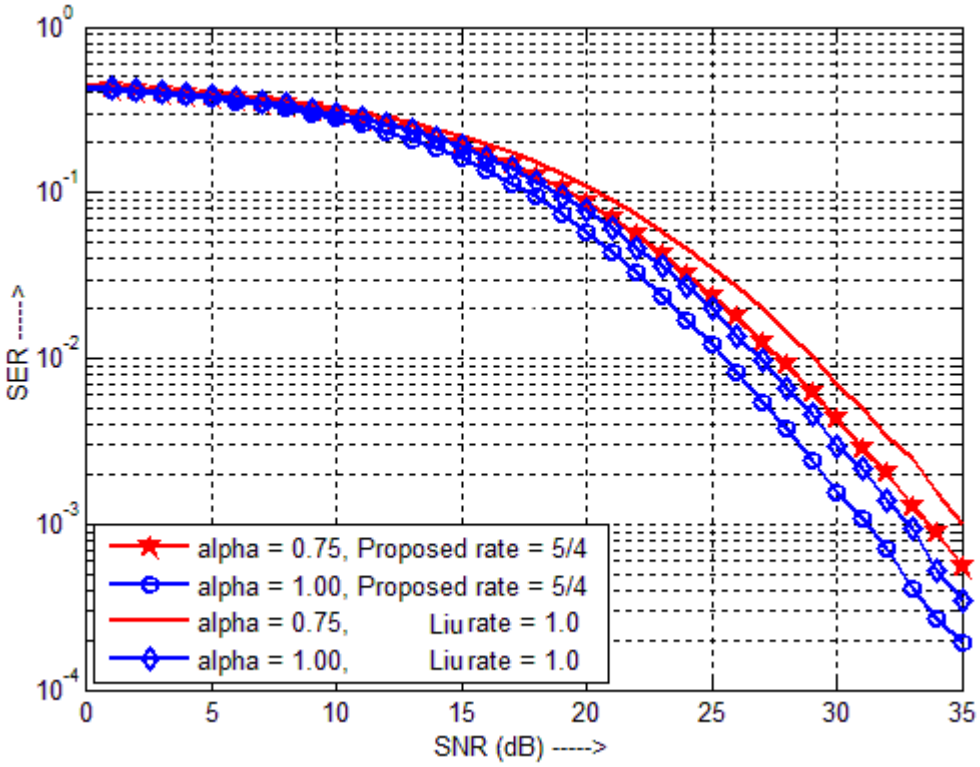


**Fig. 5.3.** SER vs. SNR for different values of $|\alpha|$.

In the case of throughput curves, we notice that at high SNR values high-rate curves crosses over the Liu rate-one system [7], thus it is justifiable to consider that we can switch between the Liu rate-one code [7] and the high-rate code to maximize the throughput at all SNR levels. It is shown in Fig. 5.2 that as $|\alpha|$ decreases, throughput also decreases. The

transmitted signal under fast-fading conditions experiences the most severe fading effects and hence is received with high errors, which is shown in the Fig. 5.2. In the Fig. 5.2 and Fig. 5.3, it is shown that $|\alpha|$ with value 1 gives the best performance.

| Parameter | Value |
|---|---|
| Modulation used | QPSK |
| Number of transmitter and receiver antennas | $2\times1$ |
| Rayleigh fading parameter, $\|\alpha\|$ | 1, 0.75 |

**Table 5.2.** System parameters for SER of $2\times1$ STBC system under perfect CSI.

Further, from Fig. 5.3 it is shown that high-rate $(5/4)$ STBC system outperforms the Liu rate-one STBC system [7]. In Fig. 5.3, we have presented the simulation results with different values of the Rayleigh fading parameter on a single graph. It is shown from the graph that $|\alpha|$ = 1 shows a significant performance advantage over α = 0.75. High-rate $(5/4)$ STBC system achieves a performance advantage of 2dB at the SER of $10^{-3}$ for $|\alpha|$ = 1. For lower SNR values, fading effects are very severe with high SER as shown in Fig. 5.3.

### 5.4.2 Performance Evaluation for Liu Rate-One and High-Rate $(5/4)$ $2\times1$ STBC System with Imperfect CSI Under Time-Selective Environment

In this section, we have presented the simulation results obtained with the imperfect knowledge of the transmission channel. The channel state estimator provides imperfect CSI at the receiver, with the estimation error of $\Delta H_k$. In Fig. 5.4 and Fig. 5.5 the results are established for the imperfect CSI at the particular value of channel estimation error variance of -7.5dB. It is shown that in Fig. 5.4 and Fig. 5.5 that the estimation error of the channel introduces error in the STBC system.

It is clear from Fig. 5.4 that the proposed scheme achieves better performance than the conventional scheme at SNR of 30dB with $|\alpha|$ = 0.5. Simulation results demonstrate that this system is favored by high SNR and low channel estimation error. It is also apparent from the proposed system that when the channel is imperfectly estimated at the receiver, the system

performance degrades significantly. Effective throughput of $(5/4)$ system reduces to 2.25; for high-rate system at SNR = 40dB, due to imperfect CSI, whereas for Liu rate-one [7] system effective throughput reduces to 1.9.

| Parameter | Value |
|---|---|
| Modulation used | QPSK |
| Number of transmitter and receiver antennas | $2\times1$ |
| Rayleigh fading parameter, $\lvert\alpha\rvert$ | 0.5 |
| Channel estimation error | -7.5dB |

**Table 5.3.** System parameters for effective throughput of $2\times1$ STBC system under imperfect CSI.

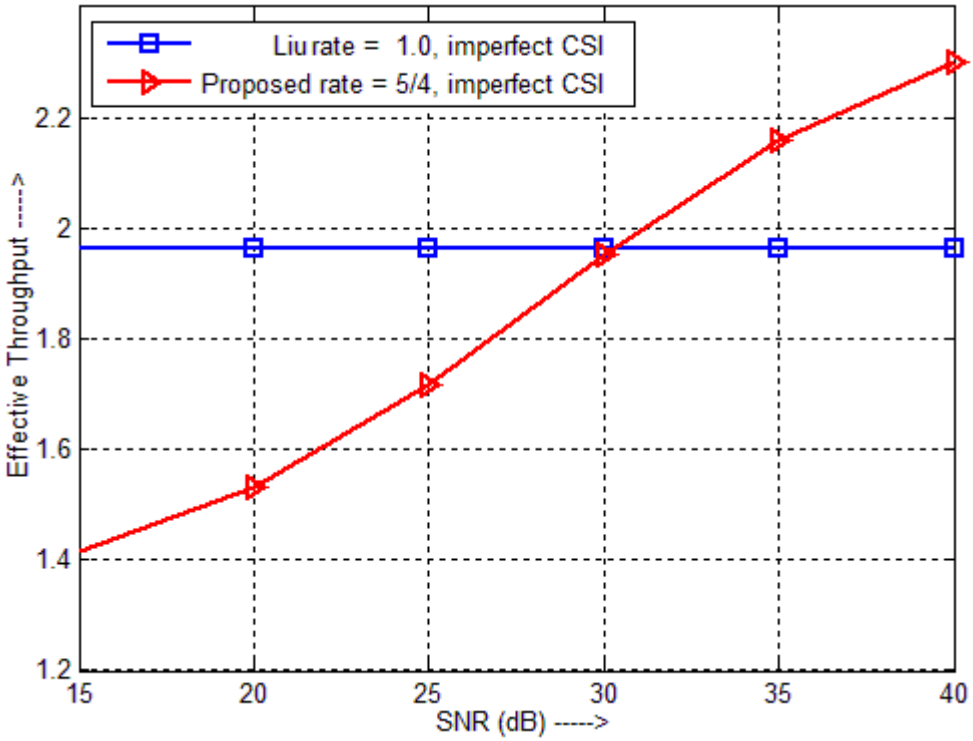


**Fig. 5.4.** Effective throughput vs. SNR under imperfect CSI with $\lvert\alpha\rvert$ =0.5.

Thus, the proposed STBC system outperforms the Liu rate-one STBC system [7] at the high SNR values, but at the cost of decoding complexity. The throughput of the high-rate ( $5/4$) STBC system supersedes the Liu rate-one STBC system [7] at approximately SNR =

30dB for the imperfect CSI case. For the SNR values higher than this crossover point, the throughput of proposed system increases with the increasing values of SNR. In case of imperfect CSI at receiver, the shift in the crossover point than the perfect CSI case indicates the adverse effects of channel estimation error on the system performance. It is shown from the curves that in the case of imperfect CSI effective throughput decrease considerably with the increase in the SER.

It is noticeable that increasing the throughput of the system also adds up the decoding errors in the system which is shown from the graphs of SER variation with SNR.

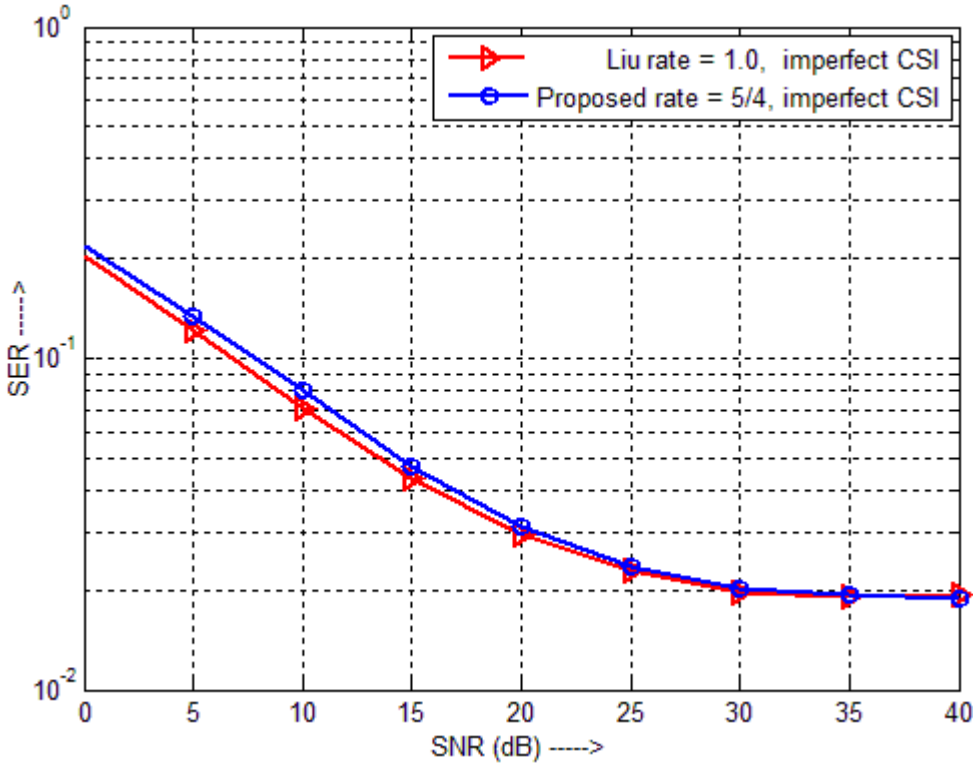


**Fig. 5.5.** SER vs. SNR under imperfect CSI with $|\alpha|$ =0.5.

For lower SNR values, the fading effects are very severe with high SER shown in Fig. 5.5. At high SNR, the performance of the system is enhanced in the case of effective throughput as well as SER. Results obtained in Fig. 5.5 depict that we are getting 1dB performance advantage in case of the high-rate curve as compared to Liu rate-one [7] curve at the SER of 0.03 for $|\alpha|$ = 1. This shows that performance advantage degrades with imperfect channel estimation. Also, at high SNR it can be shown that both schemes provide same SER performance. In Fig. 5.4 and Fig. 5.5, we have presented the simulation results with $|\alpha|$ =0.5

for Liu rate-one [7] and high-rate for the time-selective environment.

### 5.4.3 Performance Evaluation of Channel Estimation Error for Liu Rate-One and High-Rate $(5/4)$ $2\times1$ STBC System with Imperfect CSI Under Time-Selective Environment

In this section, we present the simulation results obtained with the imperfect knowledge of the transmission channel. The channel state estimator provides imperfect CSI at the receiver, with the estimation error of $\Delta H_k$.

In the Fig. 5.6 and Fig. 5.7, all the results are validated for the imperfect CSI at the specific value of SNR i.e., 7.5dB. In Fig. 5.6 and Fig. 5.7, it is shown that the deterioration in SER performance commences when channel estimation error is higher than -15dB and effective throughput also reduces as channel estimation error increases. For high error in the channel estimation, the SER and effective throughput have poor performances. As the estimation error reduces, the performance of effective throughput and SER improves significantly till it reaches a constant value.

| Parameter | Value |
|---|---|
| Modulation used | QPSK |
| Number of transmitter and receiver antennas | $2\times1$ |
| Rayleigh fading parameter, $\lvert\alpha\rvert$ | 0.5 |
| SNR | 7.5dB |

**Table 5.4** System parameters for effective throughput of $2\times1$ STBC system under imperfect CSI with fixed SNR.

It is clear from Fig. 5.6 that the proposed scheme is inferior to the conventional Liu rate-one scheme [7] at low SNR of 7.5dB with $\lvert\alpha\rvert$ = 0.5. High-rate $(5/4)$ STBC system achieves a throughput of 1.94; whereas for Liu rate-one [7] STBC system, the maximum throughput is 1.9 at the channel estimation error of -26dB. Thus, the high-rate STBC system outperforms the conventional STBC system at low channel estimation values. It is also apparent from the proposed system that when the channel is imperfectly estimated at the receiver, the system performance gets degraded significantly. In the case of imperfect CSI at receiver, the

crossover is observed at approximately -15dB in Fig. 5.6. Thus, till -15dB proposed scheme is better after which its performance degrades and at high channel estimation error conventional scheme supersedes the proposed scheme. Thus, it is shown from the numerical data that as channel estimation error increases the effective throughput reduces which indicates the adverse effects of channel estimation error on the system performance.

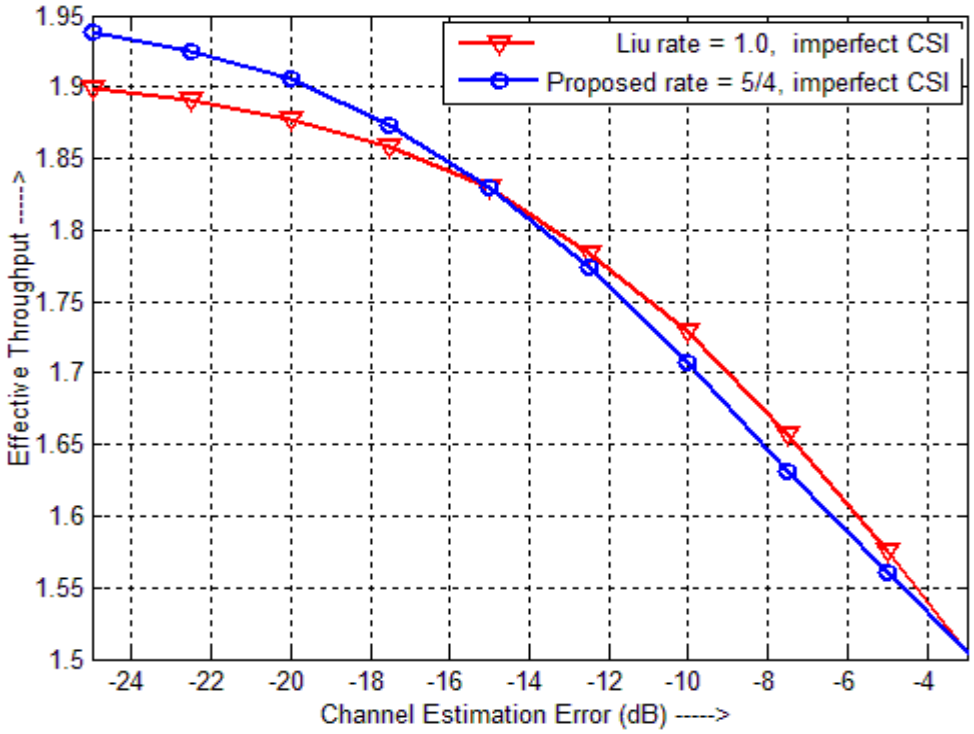


**Fig. 5.6.** Effective throughput vs. channel estimation error with $|\alpha|$ =0.5.

| Parameter | Value |
|---|---|
| Modulation used | QPSK |
| Number of transmitter and receiver antennas | $2\times1$ |
| Rayleigh fading parameter, $\|\alpha\|$ | 0.5 |
| SNR | 7.5dB |

**Table 5.5.** System parameters for SER of $2\times1$ STBC system with fixed SNR under imperfect CSI.

In Fig. 5.7, Liu rate-one scheme [7] is better than the proposed scheme in terms of SER performance. It is proved with all the results of proposed scheme that the efficiency of the

system is determined by the performance of the channel estimator. However at -20dB channel estimation error, the detrimental effects of the CSI imperfections are too low to impact the SER performance. Both the scheme approaches almost same SER performance at high channel estimation error.

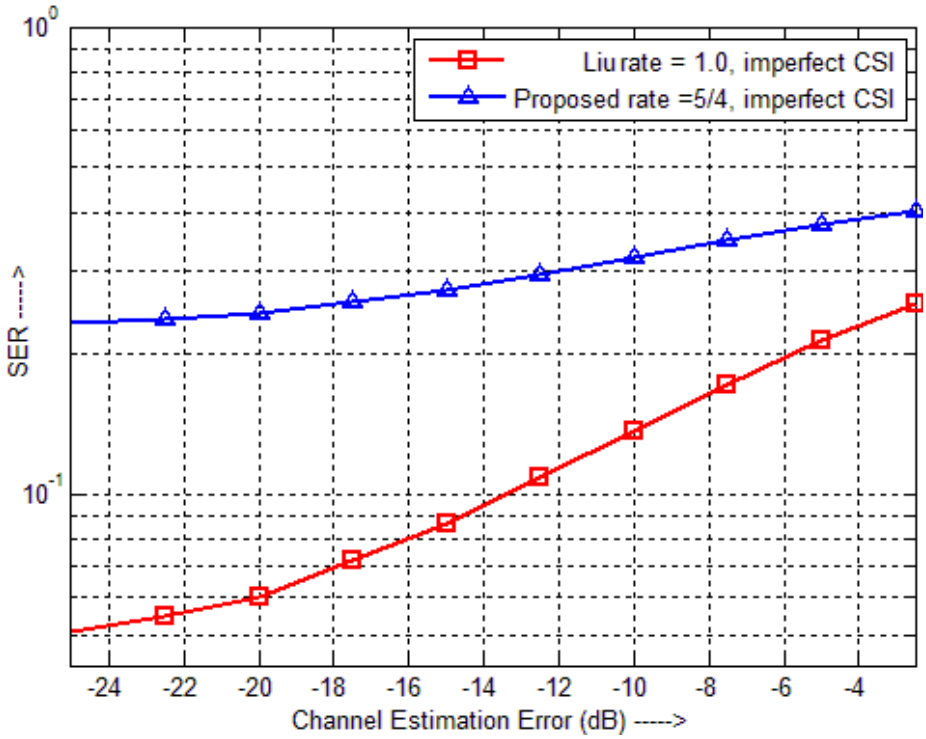


**Fig. 5.7.** SER vs. channel estimation error with $|\alpha|$ =0.5.

Thus, the performance of the proposed system depends on the performance of the channel estimator.

### 5.4.4 Performance Evaluation of High-Rate $(5/4)$ $2\times1$ STBC System with Perfect and Imperfect CSI Under Time-Selective Environment for Different Values of CFO and Doppler Frequency

*Case 1: With Different Values of CFO*

In this section, we present the simulation results in Fig. 5.8 obtained with different values of CFO when Doppler frequency has been kept constant for (5/4) rate with perfect and imperfect CSI under time-selective fading environment. Here, channel estimation error variance is considered to be -7.5dB. Further, the Doppler frequency is kept constant at 75 Hz. The value

of CFO is changed to observe the SER performance variation. Here, simulation is conducted considering $f_o T_s \Rightarrow \{0.01,\ 0.09,\ 0.2\}$, where, $f_o$ represents the carrier frequency. It is shown that reduction in the value of $f_o T_s$ favors SER.

| Parameter | Value |
|---|---|
| Modulation used | QPSK |
| Number of transmitter and receiver antennas | 2×1 |
| CFO | 0.01, 0.09, 0.20 |
| Doppler frequency | 75 Hz |
| $T_s$ | 0.001 |
| Channel estimation error | -7.5dB |

**Table 5.6.** System parameters for SER of $2\times1$ STBC system with different values of CFO.

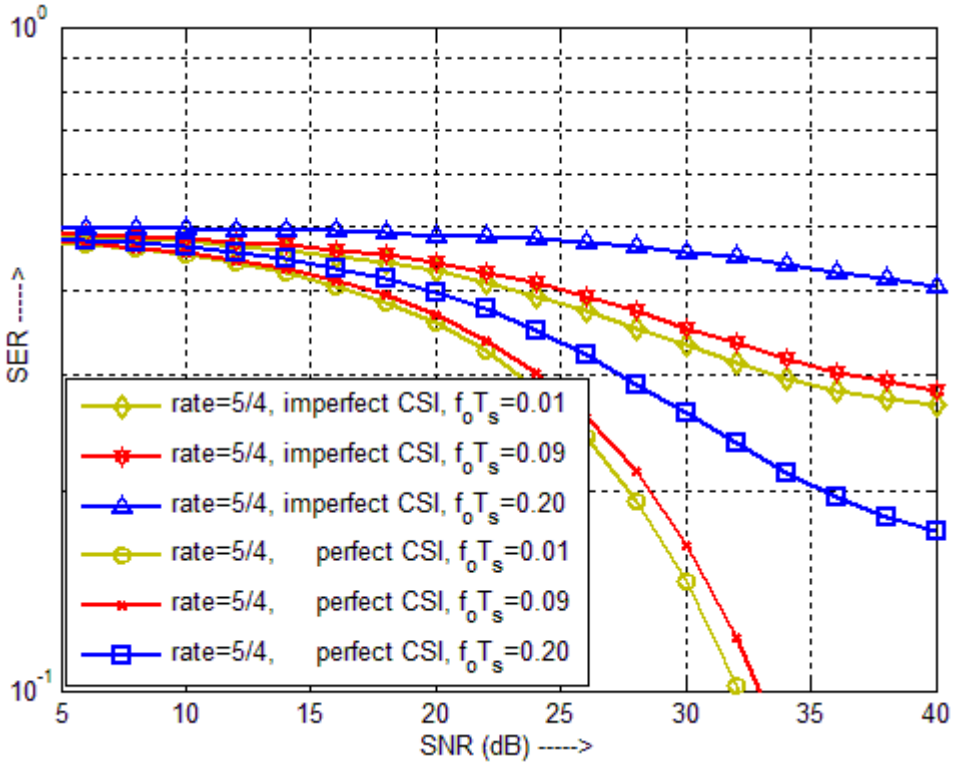


**Fig.5.8.** SER vs. SNR with different values of CFO and $f_D$ = 75Hz under perfect and imperfect CSI.

In Fig. 5.8 SER variation with SNR has been shown when Doppler frequency, $f_D$, has been kept constant at 75 Hz with the symbol period of $T_s = 0.001$. It is inferred from

simulation results in Fig. 5.8 that as the value of $f_oT_s$ is increased the SER performance of the proposed system gets degraded. It is shown that the better results are produced when the channel is perfectly estimated, such as at SNR of 35dB with CFO fixed at 0.2, SER of 0.1957 is achieved and with imperfect CSI the SER is increased to 0.4957 at the same CFO. Thus, SER performance is improved in terms of perfect channel estimation.

*Case 2: With Different Values of Doppler Frequency*

In Fig. 5.9, SER variation with SNR has been shown when CFO has been kept constant at 0.09 whereas Doppler frequency $f_D$ is fixed at 75 and 200 Hz. Here, channel estimation error has been kept at -15dB. It is shown from the graphs that at high value of fade rate i.e., $f_DT_s$ SER performance deteriorates.

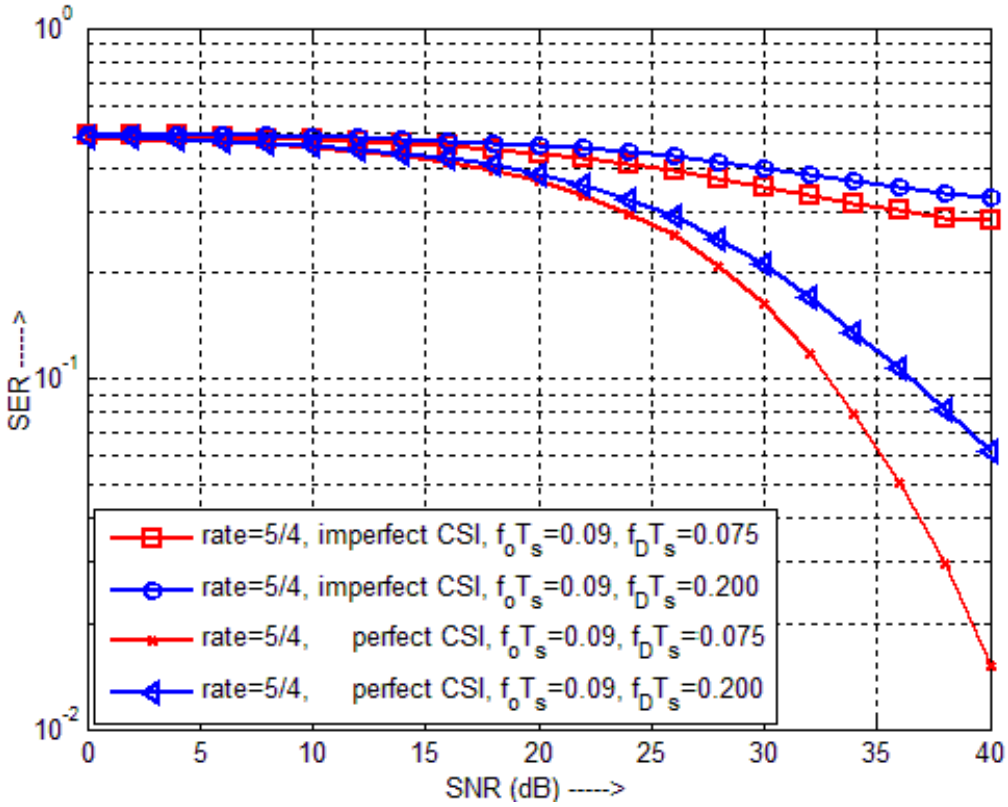


**Fig.5.9.** SER vs. SNR with CFO set at 0.09 and $f_D$ = 75Hz and 200 Hz under perfect and imperfect CSI.

In the case where $f_D$ is fixed at 75 Hz and CFO at 0.09 a SER of 0.07 is achieved under perfect channel estimation at the SNR of 35dB whereas SER is increased to 0.315 under

imperfect channel estimation. It is shown that the better results are achieved when the channel is perfectly estimated i.e., the SER performance is improved in terms of perfect channel estimation.

It is shown from the graphs and the numerical results that the better results are achieved with $f_D$ of 75 Hz in comparison to 200 Hz. Since the channel is less time-varying and the fade rate is less, better SER performance is achieved.

| Parameter | Value |
|---|---|
| Modulation used | QPSK |
| Number of transmitter and receiver antennas | $2\times1$ |
| CFO | 0.09 |
| Doppler frequency | 75 and 200 Hz |
| $T_s$ | 0.001 |
| Channel estimation error | -15dB |

**Table 5.7.** System parameters for SER of $2\times1$ STBC system with different values of Doppler frequency.

### 5.4.5 Performance Evaluation of Alamouti Rate-One and High-Rate $(9/8)$ $4\times1$ STBC System with Perfect and Imperfect CSI Under Time-nonselective Environment

- ***High-rate*** $9/8$ ***STBC communication system model***

Fig. 5.10 depicts a wireless communication system with four-transmitter antennas and one-receive antenna. Here, the information symbols are transmitted using Alamouti space-time block-coding with selective power scaling, so as to achieve high transmission rate. The channel is assumed to be Rayleigh flat-fading.

According to [1], [3], QO-STBC scheme is introduced to achieve full-rate in four-transmitter antennas at the cost of diversity-gain loss.

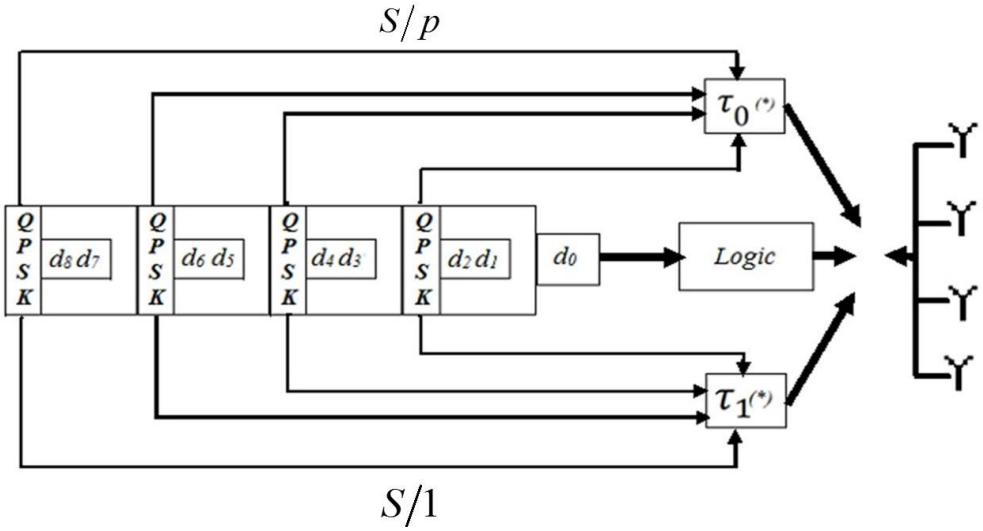


**Fig. 5.10.** Block diagram of the data-rate $9/8$ STBC system using QPSK modulation [4].

The encoding matrix for the four-transmitter antennas introduced in [5] is given as

$$S = \begin{bmatrix} S_{12} & S_{34} \\ S_{34} & S_{12} \end{bmatrix} = \begin{bmatrix} s_1 & s_2 & s_3 & s_4 \\ -s_2^* & s_1^* & -s_4^* & s_3^* \\ s_3 & s_4 & s_1 & s_2 \\ -s_4^* & s_3^* & -s_2^* & s_1^* \end{bmatrix} \tag{5.36}$$

A frame of 9 bits is considered, out of which 8 data bits are paired as $\{d_1, d_2\}, \{d_3, d_4\}, \{d_5, d_6\}, \{d_7, d_8\}$. These pairs are mapped on QPSK constellation to generate the information symbols $s_i$. The bit $d_o$ is used to decide about the selective power scaling.

In this communication system with $d_o = 0$ and power scaling by $1/p$ through $\tau_0(.)$, the four consecutive signal/symbol samples are represented as

$$S_T = \frac{S}{p} \tag{5.37}$$

where, $p > 1$

In this communication system with $d_o = 1$ and power scaling by unity through $\tau_1(.)$, the four consecutive signal/symbol samples are represented as

$$S_T = \frac{S}{1} \tag{5.38}$$

By Alamouti [1] and Jafarkhani [3], the received signal samples can be expressed in matrix form as

$$\bar{R} = \bar{H}\bar{S} + \bar{N} \tag{5.39}$$

The channel matrix [5] is derived by applying a complex conjugate operation on the second and fourth element of the received signal as

$$\bar{R} = \begin{bmatrix} r_1 \\ r_2^* \\ r_3 \\ r_4^* \end{bmatrix} = \bar{H}. \begin{bmatrix} s_1 \\ s_2 \\ s_3 \\ s_4 \end{bmatrix} + \begin{bmatrix} \eta_1 \\ \eta_2^* \\ \eta_3 \\ \eta_4^* \end{bmatrix} \tag{5.40}$$

where, $\bar{R}$ is the $4\times1$ received signal vector, $\bar{H}$ is the $4\times4$ channel matrix, $\bar{S}$ is the $4\times1$ transmitted symbol sample vector and $\bar{\mathrm{N}}$ is the additive white Gaussian noise vector with zero-mean and variance $\sigma_N^2$. Each element of matrix $\bar{H}$ is time-varying as discussed in section 5.2

- ***Matched Filtering Operation and ML Decoding***

If the channel state information is perfectly known to us [1], then the received symbols are decoded as

$$\bar{Y} = \bar{H}^H \bar{R} \tag{5.41}$$

If the channel state information is not perfectly known to us [1], [6], then the symbols are decoded as

$$\bar{Y} = \hat{H}^H \bar{R} \tag{5.42}$$

where, $\hat{H} = \bar{H} + \Delta H$ and $(.)^H$ is the Hermitian matrix operator. Here, $\Delta H$ is the channel estimation error with mean $\eta_{\Delta H} = 0$ and variance = $\sigma_{\Delta H}^2$. The simple matched filtering

operation on received signal vectors $\overline{R}$ results in two candidate solutions $\left\{\hat{S}, \frac{\hat{S}}{p}\right\}$ . These candidate solutions are then compared using ML decoding [2], [4]. This result of ML decoding thus performs the decoding of $d_o$ because the decision can be made between $\overline{S}$ or $\overline{S}/p$ .

The performance of the proposed scheme will be analyzed, while working under Rayleigh fading channel, using QPSK modulation. It is considered that the total power is equally divided by the number of transmit antennas. Here, we assume that the flat-fading channel tap-coefficients remain unaltered over four consecutive symbol periods. The receiver either has perfect or imperfect knowledge of the channel state information under different scenarios. In selective power scaling scheme, the value of $p$ is set at $\sqrt{2}$ [4].

In this section, we have presented the simulation results obtained with the perfect and imperfect knowledge of the transmission channel and compared them. The channel state estimator provides imperfect CSI at the receiver, with the estimation error of $\Delta H_k$. In Fig. 5.11, the results are established for the imperfect CSI at the particular value of channel estimation error as -14dB.

It is clear from Fig. 5.11 that the proposed scheme achieves better performance than the conventional scheme at -14dB channel estimation error variance with $|\alpha|$ = 0.5. Simulation results demonstrate that this system is favored by high SNR and low channel estimation error. It is also apparent from the proposed system that when the channel is imperfectly estimated at the receiver, the system performance gets degraded significantly. For the high signal-to-noise-ratio values, SER performance is enhanced. In case of imperfect CSI at receiver, the SER performance degrades which indicates the adverse effects of channel estimation error on the system performance.

At high SNR, we are getting 2dB performance advantage in the high-rate $9/8$ system as compared to Alamouti rate-one [1] system in terms of SER performance.

| Parameter | Value |
|---|---|
| Modulation used | QPSK |
| Number of transmitter and receiver antennas | 4×1 |
| Rayleigh fading parameter $\|\alpha\|$ | 0.5 |
| Channel estimation error | -10dB |

**Table 5.8.** System parameters for SER of $4\times1$ STBC system under imperfect CSI.

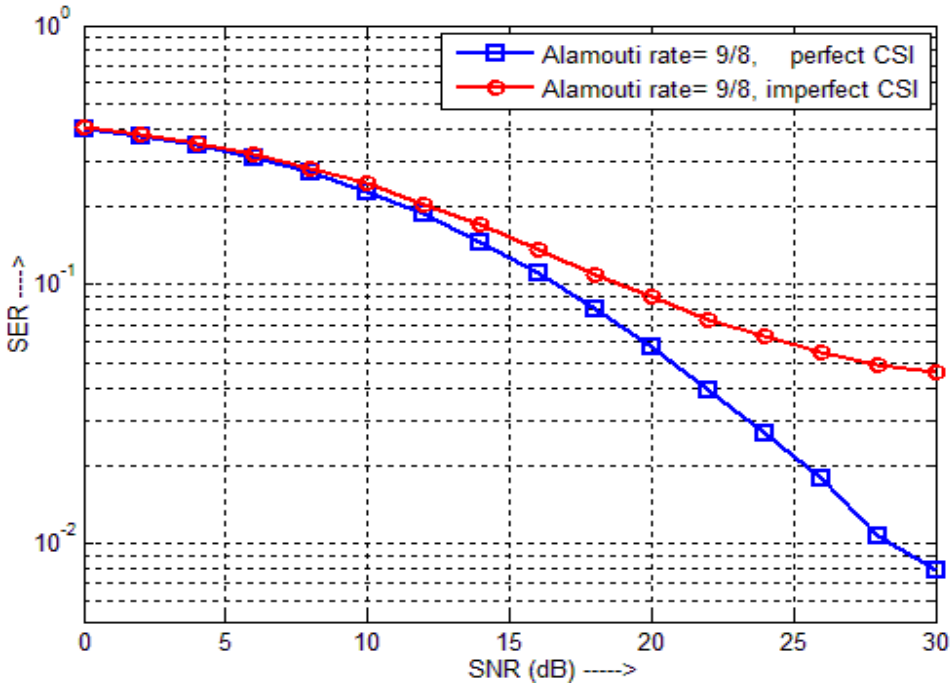


**Fig. 5.11.** SER vs. SNR under perfect and imperfect CSI with $|\alpha|$ =0.5.

| Parameter | Value |
|---|---|
| Modulation used | QPSK |
| Number of transmitter and receiver antennas | 4×1 |
| Rayleigh fading parameter $\|\alpha\|$ | 0.5 |
| SNR | 5, 10, 15dB |

**Table 5.9.** System parameters for SER of $4\times1$ STBC system with different values of SNR.

In Fig. 5.12, Alamouti high-rate STBC system for $4\times1$ has been plotted with different values of SNR and channel estimation error. It is shown from the graph that high SNR curve has better SER performance as compared to the performance at lower SNRs. The SER performance improves with the decreasing value of channel estimation error variance. The SER performance of the underlying system is found to improve with the increasing value of SNR.

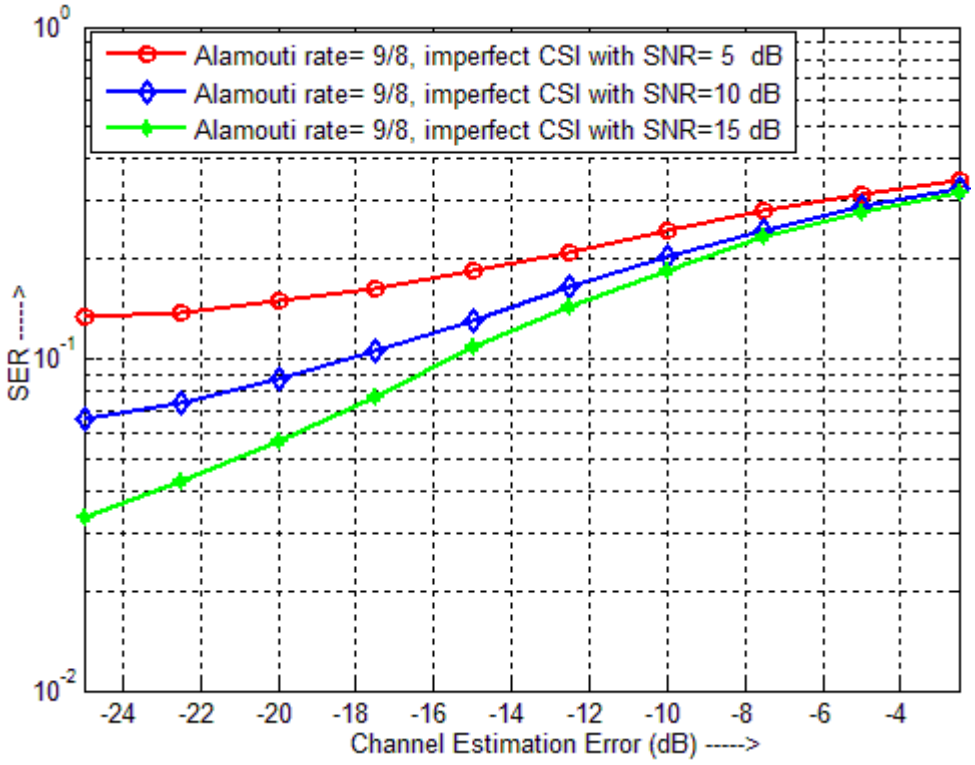


**Fig. 5.12.** SER vs. SNR with different values of SNR and channel estimation error under imperfect CSI.

Thus, it has been proven that the proposed scheme is favored by high SNR and low channel estimation error. As the channel estimation error increases in value, SER performance degrades and at the channel estimation error of -4dB, we are getting performance that is similar for all the three curves.

### 5.4.6 Performance Comparison of Alamouti Rate-One and High-Rate $(9/8)$ $4\times1$ STBC System with Different Values of CFO Under Time-nonselective Environment

It is clear from Fig. 5.13 that the proposed scheme achieves better performance than the conventional scheme at -10dB channel estimation error variance with $|\alpha|$ = 0.5 and $f_oT_s$ =

0.01. Simulation results demonstrate that this system is favored by high SNR and low channel estimation error. High-rate $9/8$ STBC system achieves a throughput of 2.25; whereas for Alamouti rate-one [1] STBC system, the maximum throughput is 2. Thus, the proposed STBC system outperforms the Alamouti rate-one STBC system [1] at the high SNR values, but at the cost of increased decoding complexity.

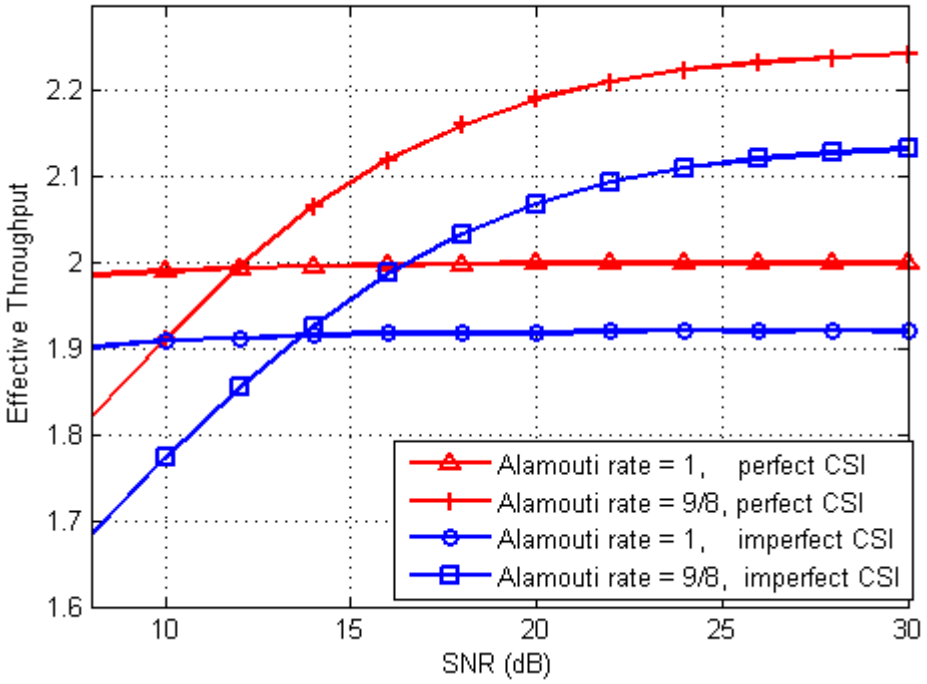


**Fig. 5.13.** Effective throughput vs. SNR at $|\alpha|$ =0.5.

| Parameter | Value |
|---|---|
| Modulation used | QPSK |
| Number of transmitter and receiver antennas | $4\times1$ |
| Rayleigh fading parameter $\|\alpha\|$ | 0.5 |
| Channel estimation error | -10Db |

**Table 5.10.** System parameters for effective throughput of $4\times1$ STBC system under imperfect CSI.

It is also apparent from the proposed system that when the channel is imperfectly estimated at the receiver, the system performance degrades significantly. Effective

throughput of $9/8$ system reduces to 2.13 for the high-rate system at SNR = 30dB, due to imperfect CSI. The throughput of the high-rate $9/8$ STBC system supersedes the Alamouti rate-one STBC system [1] at approximately SNR = 12dB for the perfect channel state information case. For the SNR values higher than this crossover point the throughput of the proposed system increases with the increasing values of SNR.

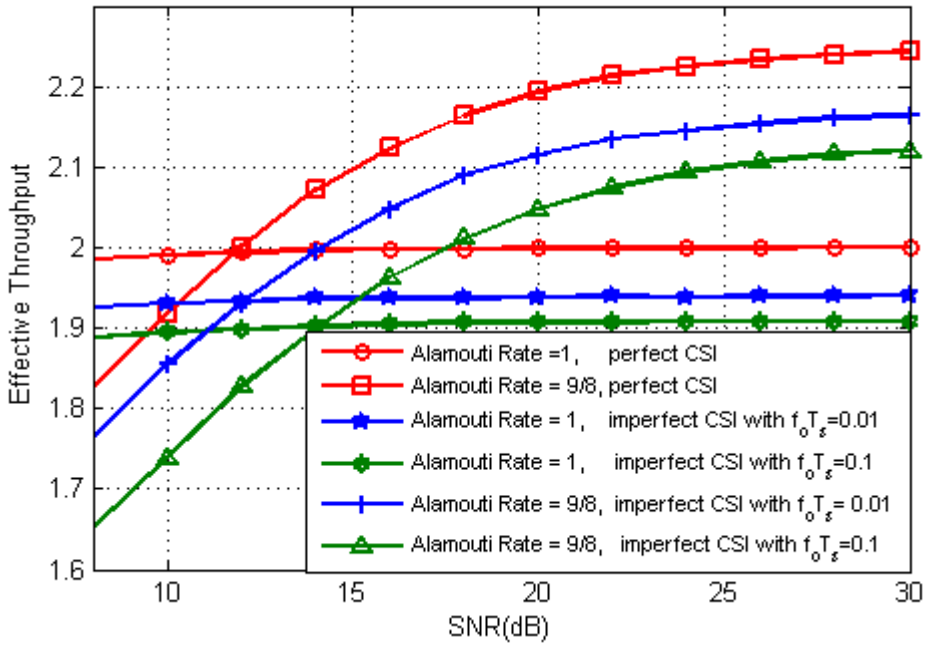


**Fig. 5.14.** Effective throughput vs. SNR at different values of CFO.

In the case of imperfect CSI at receiver, the crossover is observed at approximately 14dB in Fig. 5.14, which indicates the adverse effects of channel estimation error on the system performance. Further, the Doppler spread is kept constant at 240 Hz with $T_s = 0.001$. The channel estimation errors are considered to be -20dB. The value of CFO is changed to observe the throughput performance variation. Here, simulation is conducted considering $f_o T_s \Rightarrow \{0,\ 0.01,\ 0.1\}$. It is inferred from simulation results in Fig. 5.14 that as the value of $f_o T_s$ is increased the throughput performance of the proposed system gets deteriorated. However, beyond the crossover point the proposed high-rate $9/8$ STBC system outperforms the Alamouti rate-one STBC system [1]. Moreover, an increase in the value of $f_o T_s$ leads to an increase in the shifting of cross-over point at a higher value of SNR.

| Parameter | Value |
|---|---|
| Modulation used | QPSK |
| Number of transmitter and receiver antennas | $4\times1$ |
| CFO | 0, 0.01, 0.1 |
| Doppler frequency | 240 Hz |
| $T_s$ | 0.001 |
| Channel estimation error | -20dB |

**Table 5.11.** System parameters for effective throughput of $4\times1$ STBC system with different values of CFO.

*Chapter 6*

# CONCLUDING REMARKS AND FUTURE SCOPE

## 6.1 Concluding Remarks

Two wireless systems namely high-rate $(5/4)$ and $(9/8)$ STBC schemes have been discussed along with rate-one STBC (Liu and Alamouti) in this thesis report. We have evaluated their performances in term of SER and effective throughput under two different conditions i.e., (1) Perfect CSI at the receiver (2) Imperfect CSI at the receiver. Imperfect channel estimation can cause severe problems in the STBC system.

Simulation results in Fig. 5.2 to Fig. 5.14 show that the channel estimation method provides substantial improvement in the SER performance, when the value of Rayleigh fading parameter i.e., alpha increases. We have observed that as the carrier frequency offset parameter i.e., $f_o T_s$ decreases, the effective throughput performance substantially improves. The SER as well as effective throughput performance are also observed to improve with decreasing value of the fade rate parameter i.e., $f_D T_s$. Here, we can conclude based on simulation outcomes that the proposed scheme works best under high SNR and low channel estimation error. The scheme shows performance advantage only under favorable conditions in terms of SNR, channel estimation error, Rayleigh fading parameter, fade rate, and CFO parameter.

The simulation results depict that the channel estimator is the backbone of the high-rate $(5/4)$ and high-rate $(9/8)$ STBC systems. As the channel estimation error increases, SER performance degrades, and the effective throughput is also affected adversely. The investigation has revealed that with MISO-STBC $(9/8)$ system, better results are obtained in terms of SER and effective throughput when employed in the time-nonselective environment. It has proven to be beneficial in mitigating the effects of imperfect CSI received.

The high-rate $(5/4)$ STBC system is proposed using Liu rate-one [7] scheme in combination with selective power scaling, which works under time-selective environment. Also, the high-rate $(9/8)$ STBC system is proposed using Alamouti rate-one scheme [1]

working under time-nonselective environment. The channel estimation error undoubtedly affects the effective throughput and SER performance of the proposed STBC system. In addition to this, the carrier frequency offset plays a significant role in determining its effective throughput and SER performance. The proposed high-rate $(5/4)$ is found to outperform the conventional Liu rate-one [7], and $(9/8)$ STBC system is found to supersede the Alamouti rate-one [1] STBC system only under favorable conditions i.e., at low $f_D T_s$, low $f_o T_s$, high SNR, low channel estimation errors and high $|\alpha|$.

### 6.2 Future Scope

- The combination of imperfect channel estimation technique with different error correction decoding techniques can further improve the performance. It can also be implemented with or without perfect CSI.

- The proposed scheme can be extended for the four and eight-transmitter antenna. Future work may include to make the channel estimator work under more adverse conditions of different fading environment and also to reduce the complexity of the system.

- The extension of the presented work to STBC-OFDM systems in the presence of carrier frequency offset and channel estimation errors.

# REFERENCES


[1] S. M. Alamouti, "A simple transmit diversity technique for wireless communications," *IEEE J. Select. Areas Commun.*, vol.16, no. 8, pp. 1451-1458, October 1998.

[2] S. Das, N. Al-Dhahir, and R. Calderbank, "Novel full- diversity high-rate STBC for 2 and 4 transmit antennas," *IEEE Commun. Lett.*, vol. 10, no. 3, pp. 171-173, Mar. 2006.

[3] H. Jafarkhani, "A quasi-orthogonal space-time block code," *IEEE Trans. Commun.*, vol. 49, no. 1, pp. 1-4 , January 2001.

[4] A. Grover and A. K. Kohli, "Full diversity high-rate space-time block-coded systems using estimated channel state information for symbol detection," *Int. J. Physical Sci.*, vol. 7, no. 17, pp. 2539-2548, April 2012.

[5] U. Park, S. Kim, K. Lim, and J. Lim, "A novel QO-STBC scheme with linear decoding for three and four transmit antennas," *IEEE Commun. Lett.*, vol. 12, no. 12, pp. 868-870, December 2008.

[6] A. Bansal and A. K. Kohli, "Suppression of impulsive noise in OFDM system using imperfect channel state information," *Elsevier, Int. J. Light and Elect. Optics*, vol. 127, no. 4, pp. 2111-2115, February 2016.

[7] Z. Liu, X. Ma, and G. B. Giannakis, "Space-time coding and Kalman filtering for time-selective fading channels," *IEEE Trans. Commun.*, vol. 50, no. 2, pp. 183-186, February 2002.

[8] T. S. Rappaport, *Wireless Communications*, 3rd ed., Upper Saddle River, NJ: Prentice Hall, 1996.

[9] W. C. Jakes, *Microwave Mobile Communication*, 2nd ed., New York, NY: Wiley, 1974.

[10] Athanasios Papoulis, *Probability Random Variables and Stochastic Processes*, 4th ed., West Patel Nagar, ND: Tata McGraw-Hill, 1995.

[11] W. Su and X. G. Xia, "Signal constellations for quasi-orthogonal space-time block codes with full diversity," *IEEE Trans. Inform. Theory*, vol. 50, no. 10, pp. 2331-2347, October 2004.

[12] M. Zhuang, "Effects of erroneous CSI on the performance of multiple-transmit antenna selection," *Int. J. Antenna Propag.*, vol. 2015, pp. 1-13, 2015.

[13] V. Tarokh, N. Seshadri, and A. R. Calderbank, "Space-time codes for high data rate wireless communications: performance criterion and code construction," *IEEE Trans. Inform. Theory*, vol. 44, no. 2, pp. 744-765, March 1998.

[14] T. Xing, Y. Wang, Y. Zhan, and J. Lu, "4-transmit-antenna STBC with 1-bit differential feedback over time-selective fading channels," *IEEE Int. Conf. Commun.*, pp. 1-5, May 2010.

[15] W. Gappmair and M. Bergmann, "Estimation of carrier and channel parameters in time-selective fading channels," *IET Commun.*, vol. 9, no. 12, pp. 1474-1478, August 2015.

[16] S. N. Diggavi, N. Al-Dhahir, A. Stamoulis, and A. R. Calderbank, "Differential space-time coding for frequency-selective channels." *IEEE Commun. Lett*, vol. 6, no. 6, pp. 253-255, June 2002.

[17] V. Tarokh, A. Naguib, N. Seshadri, and A. R. Calderbank, "Space-time codes for high data rate wireless communication: performance criteria in the presence of channel estimation errors, mobility, and multiple paths," *IEEE Trans. Commun.*, vol. 47, no. 2, pp. 199-207, February 1999.

[18] A. Goldsmith, *Wireless Communcations*, 2nd ed., West 20th Street, NY: Cambridge University Press, 2005.

[19] A. K. Kohli, "Fading model for antenna array receiver for a ring-type cluster of scatterers," *Taylor & Francis, Int. J. Electron.*, vol. 98, no. 7, pp. 933- 940, July 2011.

[20] H. Taub, D.L. Schilling, and G. Saha, *Principles of Communication Systems*, 3rd ed. West Patel Nagar, ND: Tata McGraw-Hill, 2008.

[21] G. J. Foschini and M. J. Gans, "On the limits of wireless communication when using multiple antennas," *Springer, Wireless Person. Commun.*, vol. 6, no. 3, pp. 311-335, March 1998.

[22] T. Shahriad, N. Farheen, and A.K.M. Alam, "Performance analysis of a microwave link using space-time block code (STBC) with receiver diversity," *Int. J. Sci Eng. Res.*, vol. 4, no. 11, November 2013.

[23] A. Molish, *Wireless Communcations*, 1st ed., West Sussex, UK: John Wiley & Sons Ltd., 2005.

[24] J. H. Winters, "On the capacity of radio communications systems with diversity in Rayleigh fading environments," *IEEE J. Select. Areas Commun.*, vol. 5, no. 5, pp. 871-878, June 1987.

[25] R. S. Blum and J. H. Winters, "On optimum MIMO with antenna selection," *IEEE Commun. Lett.*, vol. 6, no. 8, pp. 322-324, August 2002.

[26] S. Haykin, *Communication Systems*, 4th ed., Prentice Hall, NY: John Wiley & Sons Ltd., 2001.

[27] B. Hassibi and B. M. Hochwald, "High-rate codes that are linear in space and time,"

*IEEE Trans. Inform. Theory*, vol. 48, no. 7, pp. 1804-1824, August 2002.

[28] A. F. Naguib, "On the matched filter bound of transmit diversity techniques," *IEEE Int. Conf.*, vol. 2, pp. 596-603, June 2001.

[29] W.C. Lindsey and M.K. Simon, *Telecommunication Systems Engineering,* 2nd ed., Prentice Hall, Inc., NJ: Englewood Cliffs, 1973.

[30] H. Arslan and G. E. Bottomley, "Channel estimation in narrowband wireless communication systems," *Wireless Commun. Mobile Comput.*, vol. 1, no. 2, pp. 201-219, April-June 2001.

[31] I. E. Telatar, "Capacity of multi-antenna Gaussian channels," *AT&T Bell Labs.*, Tech. Rep., 1995.

[32] Y. M. Khattabi and M. M. Matalgah, "Performance analysis of multiple-relay AF cooperative systems over Rayleigh time-selective fading channels with imperfect channel estimation," *IEEE Trans. Veh. Tech.*, vol. 65, no. 1, pp. 427- 434, February 2015.

[33] Q. Zhao and H. Li, "Performance of differential modulation with wireless relays in Rayleigh fading channels," *IEEE Commun. Lett.*, vol. 9, no. 4, pp. 343-345, April 2005.

[34] X. Ma and G. B. Giannakis, "Space-time coding for doubly selective channels," *Proc. Int. Symp. Circuits Syst.*, vol. 3, pp. 647-650, May 2002.

[35] G. B. Giannakis and C. Tepedelenlioglu, "Basis expansion models and diversity techniques for blind identification and equalization of time-varying channels," *Proc. IEEE*, vol. 86, no. 10, pp. 1969-1986, October 1998.

[36] J. Mietzner, P. A. Hoeher, and M. Sandell, "Compatible improvement of the GSM/EDGE system by means of space-time coding techniques," *IEEE Trans. Wireless Commun.*, vol. 2, no. 4, pp. 690-702, July 2003.

[37] C. B. Papadias and G. J. Foschini, "Capacity-approaching space-time codes for systems employing four transmitter antennas," *IEEE Trans. Inform. Theory*, vol. 49, no. 3, pp. 726-733, March 2003.

[38] E. Lindskog and A. Paulraj, "A transmit diversity scheme for channels with interference," *Proc. IEEE ICC,* New Orleans, LA, vol. 1, no. 8, pp. 307-311, June 2000.

[39] B. Badic, M. Herdin, G. Gritsch, M. Rupp, and H. Weinrichter, "Performance of various data transmission methods on measured MIMO channels," *59$^{th}$ IEEE Veh. Tech. Conf. VTC Spring*, Milan, Italy, vol. 2, May 2004.

[40] T. Ramaswamy, K. C. Reddy, and M. Divyasri, "Space-time block coding (STBC) for multiple transmit antennas over time-selective fading channels," *Int. J. Comp. App.*, vol. 130, no. 12, pp. 38-45, November 2015.

[41] F. C. Zheng and A. G. Burr, "Receiver design for orthogonal space-time block coding for four transmit antennas over time-selective fading channels," *Proc. IEEE Globecom*, San Francisco, CA, vol. 1, pp. 128-132, December 2003.

[42] T. A. Tran and A. B. Sesay, "A generalized simplified ML decoder of orthogonal space-time block code for wireless communications over time-selective fading channels," *Proc. IEEE Veh. Tech. Conf.,* vol. 3, pp. 1911-1915, May 2002.

[43] F. C. Zheng and A. G. Burr, "Signal detection for non-orthogonal space-time block coding over time-selective fading channels," *IEEE Commun. Lett.,* vol. 8, no. 8, pp. 491-493, August 2004.

[44] D. Kumar and A. K. Kohli, “Detection of high-rate STBC in frequency selective m-Nakagami fading environment,” *Int. J. Eng. Res. Gen. Sci.,* vol. 2, no. 4, pp. 1-9, July 2014.

[45] N. C. Beaulieu and C. Cheng, “Efficient Nakagami-m fading channel simulation,” *IEEE Trans. Veh. Tech.*, vol. 54, no. 2, pp. 413-424, March 2005.

[46] S. V. Vaseghi, *Advance Digtial Signal Processing and Noise Reduction*, 2nd ed., John Wiley & Sons, 2000.

[47] M. Z. A. Khan and B. S. Rajan, “Single-symbol maximum likelihood decodable linear STBCs,” *IEEE Trans. Inf. Theory*, vol. 52, no. 5, pp. 2062-2091, May 2006.

[48] D. S. Kapoor and A. K. Kohli, “Simulation of basis expansion model for channel fading using AR1 process,” *Springer, Wireless Person. Commun.*, vol. 85, no. 3, pp. 791-798, December 2015.

[49] E. Basar and U. Aygolu, “ High rate full diversity space-time block codes for three and four transmit antennas,” *IET Commun.,* vol. 3, no. 8, pp. 1371-1378, January 2009.

[50] B. Badic, P. Fuxj ager, and H. Weinrichter, “Optimization of coded MIMO-transmission with antenna selection,” *IEEE Veh. Tech. Conf.,* Sweden, vol. 2, pp. 905-909, May 2005.

# LIST OF PUBLICATIONS

[1] S. Garg and A. K. Kohli, "Impact of carrier frequency offset on throughput performance of high-rate STBC system," *Elsevier, Optik-Int. J. Light Electron Optics*, Under Review, 2016.

# 801463027

*by* Sonali Garg

| | | | |
|---|---|---|---|
| FILE | 801463027.PDF (1.64M) | | |
| TIME SUBMITTED | 02-JUL-2016 11:21AM | WORD COUNT | 16734 |
| SUBMISSION ID | 687507599 | CHARACTER COUNT | 86318 |

801463027

ORIGINALITY REPORT

| 15% | 3% | 10% | 8% |
|---|---|---|---|
| SIMILARITY INDEX | INTERNET SOURCES | PUBLICATIONS | STUDENT PAPERS |

PRIMARY SOURCES

| | | |
|---|---|---|
| 1 | Submitted to Thapar University, Patiala<br>Student Paper | 4% |
| 2 | Gaudenzi, M.. "Fucík Spectrum for a Third Order Equation", Journal of Differential Equations, 19960701<br>Publication | 1% |
| 3 | S. Das. "Novel full-diversity high-rate STBC for 2 and 4 transmit antennas", IEEE Communications Letters, 3/2006<br>Publication | 1% |
| 4 | Park, Unhee, Sooyoung Kim, Kwangjae Lim, and Jing Li. "A novel QO-STBC scheme with linear decoding for three and four transmit antennas", IEEE Communications Letters, 2008.<br>Publication | 1% |
| 5 | Bansal, Abhishek, and Amit Kumar Kohli. "Suppression of impulsive noise in OFDM system using imperfect channel state information", Optik - International Journal for Light and Electron Optics, 2016.<br>Publication | <1% |